IRis

Northeastern University

Physics Dissertations

Department of Physics

January 01, 2009

Experimental implications of static and dynamic Casimir effect instabilities.

Pradeep Ganesh Murugesan
Northeastern University

Recommended Citation

Murugesan, Pradeep Ganesh, "Experimental implications of static and dynamic Casimir effect instabilities." (2009). *Physics Dissertations.* Paper 2. http://hdl.handle.net/2047/d10018499

This work is available open access, hosted by Northeastern University.

Experimental Implications of Static and Dynamic Casimir Effect Instabilities

A dissertation presented

by

Pradeep Ganesh Murugesan

to
The Department of Physics

In partial fulfillment of the requirements for the degree of

Doctor of Philosophy

in the field of

Physics

Northeastern University

Boston, Massachusetts

April, 2009

Experimental Implications of Static and Dynamic Casimir Effect Instabilities

by

Pradeep Ganesh Murugesan

ABSTRACT OF DISSERTATION

Submitted in partial fulfillment of the requirements
for the degree of Doctor of Philosophy in Physics
in the Graduate School of Arts and Sciences of
Northeastern University, April 2009.

ABSTRACT

When fluctuating electromagnetic fields in vacuum couple strongly with matter, under certain conditions, thermodynamic instability can arise. A general theoretical framework which addresses this problem is derived, in this thesis. A deep connection is shown to exist between 'scattering phase shifts', 'bound states' and 'thermodynamic instabilities'. The emergence of such instability in a ferroelectric composed of spin zero particles, interacting strongly with photons via electric dipole interactions, is thoroughly examined.

When the field modes are modulated, under certain resonant conditions, theory predicts spontaneous generation of photons from the vacuum. The number of photons as predicted by such theories, diverge exponentially with the modulation. A general theoretical formalism which resolves this instability is provided in the thesis. The proposed experiment to detect dynamic Casimir effect, is modeled within this framework, and the number of photons that would be produced in the experiment is estimated.

ACKNOWLEDGEMENTS

I would like to thank my mentor, Prof. Allan Widom, for patiently guiding me through my thesis work. Being his student has been an immensely enriching experience for me.

I'm very grateful to Prof. Yogendra Srivastava for all his support.

My sincere thanks to the Department of Physics for providing me with the financial assistance during my doctoral work.

I'm very thankful to Northeastern University library for its fabulous resources.

I will be indebted, all my life, to my parents, for their love and sacrifice.

Contents

Abstract **2**

Acknowledgements **4**

1 Introduction **1**

2 Static Casimir Effect **7**

2.1 History 7

2.1.1 Theoretical Considerations 7

2.1.2 Experimental Tests 11

2.2 Static Casimir Effect Stability 17

2.2.1 Polarization Effects and Ferro-electricity 17

2.2.2 General Theory 21

2.2.3 Application to Bulk Matter 26

2.3 Ferroelectric Phase Transitions 28

2.3.1 General Formalism 28

2.3.2 Free Energy Calculations for Spin Zero System 30

3 Dynamic Casimir Effect **39**

3.1 History 39

3.1.1 Theoretical Considerations 39

3.1.2 Experimental Difficulties and Recently Proposed Dynamic Casimir Effect Experiment 46

3.2 General Theory 48

3.2.1 Lagrangian Circuit Description 48

3.2.2 Oscillator Circuit Damping 50

3.2.3 Dynamical Casimir Effects 52

3.2.4 Periodic Frequency Modulation 55

3.3 Application to the Proposed Cavity Experiment 58

3.3.1 Photon Generation Rates 58

3.3.2 Calculation of Frequency Shifts in the Cavity 63

3.3.3 Theoretical Dynamical Casimir Effect Instability 69

3.3.4 Restoration of Theoretical Stability 70

3.3.5 Calculations and Predictions 73

4 Conclusions **75**

Bibliography **77**

Chapter 1

Introduction

Scientific history is punctuated with numerous moments when exotic physical theories which are in complete discord with ones visceral perception of nature, have triumphed in explaining physical phenomena which were incomprehensible using the then existing physical theories, and thereby either subsumed or replaced them. While the oft-quoted examples are the special and general relativity, and, superposition and uncertainty principles from quantum mechanics, it might not be outlandish to suggest, to append Casimir effect to this list. Though it isn't quite in league with the other entries in their effect in complete restructuring of our physical theories, it is arguably equally counter-intuitive. It completely alters our impression of vacuum as empty and inconsequential.

The notion of vacuum isn't a highbrow concept confined just to the circles of scholarly and erudite, but its one of those ideas that is so deep rooted in public consciousness that questioning their validity borders either on insanity or on impertinence. Nonetheless, popularity of an idea or sanctity of a belief doesn't automatically exempt it from scientific scrutiny. Upon careful reconsideration, Casimir demonstrated that vacuum isn't dead and insipid but posed the possibility of affecting the physi-

cal world in ways we can observe. He showed that two parallel, neutral conducting plates in vacuum attract one another, and thereby established that fluctuating quantum fields, a direct fall out of uncertainty principle, the presence of which has long been asserted by quantum field theory but has always been swept under the rug deeming it ineffectual, can lead to measurable physical consequences.

In our present Nano and MEMS era, Casimir effect has gained relevance to practical applications more than ever and not just remains as a curious offshoot of uncertainty principle because, at such fine length scales, Casimir forces are ubiquitous and its effects can no longer be ignored. Applications aside, if one embarks just on the quest for understanding the deeper machinations of nature, the quintessential spirit of our scientific culture, Casimir effect offers a plethora of fascinating problems to investigate.

Static Casmir Effect:

Vast amount of literature exists on static Casimir effect and a comprehensive review of all of them would require a tome in itself, if not many. So, in cutting through the thicket of morass and selecting results to be included in here, I have adopted a few guidelines. A result will be included if it is

a) a landmark result which literally brought forth the field into its existence

b) a result which illustrates unique features of Casimir effect

c) of contemporary experimental relevance.

Casimir's original result which showed the existence of an attractive force between two parallel, neutral conducting plates is outlined. Casimir forces for spherical and rectangular cavities are discussed. These results illustrate the strong dependence of the sign of the force on the geometry. All of the contemporary experiments use either flat plate-spherical lens or parallel plate geometry for measuring Casimir force.

Hence thermal, roughness and conductivity corrections to the force for these two geometries are given. All of the above are described in Sec.(2.1.1).

Experimental measurement of Casimir force has been notoriously difficult because, the forces become perceptible only at submicroscopic lengths and controlled measurement technologies at these length scales have been nonexistent until recently. Despite the serious limitations, several experimentalists have made valiant attempts in measuring Casimir force and the earliest such effort can be traced back to that of Sparnaay. Though Sparnaay was the first to measure Casimir force, his results were not conclusive. The experiment which unequivocally demonstrated the existence of Casimir force was done by Overbeek and Fockland. These two experiments are briefly discussed in Sec.(2.1.2).

With the advent of SEMs, STMs and AFMs we have begun to see and measure, control and manipulate nature at its most fundamental level, and its wake hasn't left 'Casimir effect measurements' unruffled. The first high precision measurement of Casimir force which led to resurgence in experiments related to Casimir effects, was done by Larmareaux . Subsequently, Mohideen.et.al. improvised on Larmoreax's results by incorporating thermal, roughness and finite conductivity corrections. The geometry considered in both these experiments is that of flat plate-spherical lens configuration, because, unlike the parallel plate geometry, one doesn't have to confront the daunting task of aligning the plates parallel to each other at microscopic distance of separation. Very recently, Bressi.et.al. have succeeded in measuring Casimir force for the parallel plate configuration using MEMS techniques. Complete descriptions of these three results are provided in Sec.(2.1.2).

Having given a brief overview of the history of Casimir effect, with due attention to necessary details and accuracy, our central result which explores the thermodynamic stability issues in static Casimir effect is brought into spotlight in Sec.(2.2). At

the risk of being shallow and imprecise, one might attempt to provide a heuristic explanation of the process in hand, the operative word here is heuristic - when longitudinal photon modes couple strongly with matter, thermodynamic instability can ensue signaling a phase transition. A rigorous mathematical treatment on the other hand, unearths deep connections between 'scattering phase shifts', 'bound states' and 'thermodynamic instability'. The general formalism is elaborated in Sec.(2.2.2). The interpretation of the thermodynamic instability in terms of the bulk properties of matter is provided in Sec.(2.2.3).

A detailed examination of the emergence of thermodynamic instability in a specific two state system, a ferroelectric composed of spin 0 particles and interacting strongly with photons via electric dipole interaction, is done in Sec.(2.3). The critical temperature at which the system becomes thermodynamically unstable is calculated and it is shown that the stability is restored in the system below the critical temperature, by shifting to a polarized phase.

Dynamic Casimir effect:

A quick survey of literature in dynamic Casimir effect shows that it isn't as overwhelming as its static counterpart and yet it is rich in its own right. Hence, I've included almost all the results which were truly instrumental in pushing the envelope, while those which merely trimmed and polished already existing results have been omitted. The seminal paper which flagged off the flurry of research activity which dynamic Casimir effect enjoyed was due to Yablanovitch, which proposed a new method to detect Unruh-Davis-Fulling radiation - the thermal radiation produced by an accelerating mirror in vacuum. Subsequently Lambrecht considered the problem of photon generation due to periodic oscillations of one and two parallel mirrors, and obtained an expression for the number of photons produced in the

cavity. A similar problem for the case for three dimensional cavities was addressed by Sassaroli et al. Later, Dodonov considered the effect of fluctuations in phase of the oscillations, in photon generation. All these results are detailed in Sec.(3.1.1).

Unlike static Casimir effect which has been verified to high degrees of accuracy, dynamic Casimir effect has not even been detected, let alone testing its accuracy by juxtaposing it with theoretical predictions. With all the modern sophisticated instruments at one's disposal, what looked formidable a couple of decades ago when the theoretical research was in its incipient stage, now appears to be at best elusive. The singular constraint that has been deterring experimentalists is the 'giga-hertz resonance condition' that is required to generate detectable number of photons. These difficulties are briefly discussed in Sec.(3.1.2).

An experimental group in Italy has come up with a novel method which circumvents all the hurdles that had been impeding and poses great promise of rescuing us from this impasse. The hopeless despair that had engulfed the experimental community for a long time, is now wearing thin and a waft of optimism is floating around. A complete description of the experiment is provided in Sec.(3.1.2).

If one attempts to model the experiment using the current theories, one would quickly realize that the system is exponentially unstable - the number of photons as predicted by these theories is simply too large to be physically plausible. Our central goal is to provide a theoretical framework which resolves this stability issue. The strategy is to obtain the photon generation rate equation using one of the existing theories, and then provide a fix by incorporating new 'stabilizing terms'.

Sassaroli.et.al's theory is used in obtaining the rate equation and therefore is quickly reviewed in Sec.(3.3.1). Results needed to connect the theory with the experiment are provided in Sec.(3.3.2) and the inherent instability is exposed in Sec.(3.3.3). The theoretical formalism which resolves the instability is provided in Sec.(3.3.4). As a

gesture of reassurance, a concrete numerical example is considered in Sec.(3.3.5) and is shown to yield physically meaningful results.

Chapter 2

Static Casimir Effect

2.1 History

2.1.1 Theoretical Considerations

Casimir[1],[2] first showed that two infinite parallel conducting plates attract one another due to the presence of vacuum fields. The presence of conduction plates, leads to the boundary condition on the surface of the plates

$$\mathbf{E_t} = \mathbf{H_n} = \mathbf{0} \tag{2.1}$$

This results in the fact that only certain modes of the photons can exist between the plates. The mode frequencies are given by

$$\omega_k = c\sqrt{k_1^2 + k_2^2 + \left(\frac{n\pi}{a}\right)^2} \tag{2.2}$$

The contribution of the modes to the vacuum energy is given by

$$E_{modes} = \frac{\hbar}{2} \int \frac{dk_1 dk_2}{(2\pi)^2} \sum \omega_k e^{-\delta\omega_k} S \tag{2.3}$$

where S is the area of the parallel plates and δ is the regularization parameter. The renormalization of the energy is done by subtracting the contribution of the vacuum energy that would have been present in the space between the parallel plates had the plates been absent which is given by

$$E_{space} = \frac{\hbar}{2} \int \frac{dk_1 dk_2 dk_3}{(2\pi)^3} \sum \omega_k e^{-\delta\omega_k} 2aS \tag{2.4}$$

Hence the renormalized energy is

$$E_{renorm} = E_{modes} - E_{space} \tag{2.5}$$

The summation and the integral from Eqs.(2.3), (2.4) and (2.5) can be converted into a pure integral using the Abel-Plana formula[3]. Once the integral is evaluated one gets the expression for the renormalized energy between the plates as

$$E_{renorm} = -\frac{c\hbar\pi^2}{720a^3} S \tag{2.6}$$

which yields a force given by

$$F(a) = -\frac{\partial E_{renorm}}{\partial a} = -\frac{\pi^2}{240} \frac{\hbar c}{a^4} S \tag{2.7}$$

A similar calculation for the case of dielectric plates has also been obtained wherein the force is attractive and the magnitude depends on the nature of the dielectric media[4].

The Casimir force between a metal sphere of radius R and a plate separated by a

distance d has been calculated[5] to be

$$F(d) = -\frac{\pi^3}{360} R \frac{\hbar c}{d^3} \tag{2.8}$$

In the case of a rectangular cavity[6], the nature of the force depends on the dimensions of the cavity. For a cavity with square cross-section ($a_1 = a_2 \leq a_3$) the casimir energy is given by

$$E_{renorm} \approx \frac{\hbar c}{a_1} \left[\frac{\pi}{24} - \left(\frac{\pi^2}{720} + \frac{\zeta(3)}{16\pi} \right) \frac{a_3}{a_1} \right] \tag{2.9}$$

and when ($a_1 = a_2 \geq a_3$) the casimir energy is given by

$$E_{renorm} \approx \frac{\hbar c}{a_1} \left[\frac{\pi}{48} - \frac{\zeta(3)}{16\pi} - \frac{\pi^2}{720} \left(\frac{a_3}{a_1} \right)^3 + \frac{\pi}{48} \frac{a_1}{a_3} \right] \tag{2.10}$$

Hence the energy is positive if

$$0.408 < \frac{a_3}{a_1} < 3.48 \tag{2.11}$$

and negative outside the interval. It is zero at the end of the interval.

Casimir energy for a sphere as been calculated[7] and and it is found to be positive. Review of Casimir forces calculation in various other geometries can be found in[8].

Corrections in Casimir force due to finite conductivity, thermal effects and roughness have also been calculated. The finite temperature correction to Casimir force between two parallel conductors[9],[10] in asymptotic limits $T/T_{\text{eff}} \ll$ and $\gg 1$ where $T_{\text{eff}} = \hbar c/(2a)$ are

$$F^T(a) \approx F^0(a) \left[1 + \frac{1}{3} \left(\frac{T}{T_{\text{eff}}} \right)^4 \right] \quad \text{where} \quad \text{T/T}_{\text{eff}} \ll 1 \tag{2.12}$$

and

$$F^T(a) \approx -\frac{k_B T}{4\pi a^3}\zeta_R(3) \quad \text{where} \quad \mathrm{T/T_{eff}} \gg 1 \tag{2.13}$$

The finite conductivity corrections to the parallel conductors[11],[12] is given by

$$\begin{aligned} F^C(a) \;\approx\; F^0(a)\Bigg[1 - \frac{16}{3}\frac{\delta_0}{a} + 24\left(\frac{\delta_0}{a}\right)^2 - \frac{640}{7}\left(1-\frac{\pi^2}{210}\right)\left(\frac{\delta_0}{a}\right)^3 + \\ +\frac{2800}{9}\left(1-\frac{163\pi^2}{7350}\right)\left(\frac{\delta_0}{a}\right)^4\Bigg] \end{aligned} \tag{2.14}$$

where $\delta_0 = \lambda_p/(2\pi)$ and $\lambda_p = 2\pi c/\omega_p$ where $\omega_p = 4\pi N e^2/m^*$ is the plasma frequency.

Roughness on the plates at $z = 0$ and $z = a$ are defined by,

$$z = A_1 f_1(x,y) \quad \text{and} \quad z = A_2 f_2(x,y) \tag{2.15}$$

respectively. The correction to the Casimir force between the two parallel plates due to this roughness[13] is given by

$$\begin{aligned} F^R(a) \;\approx\; F(a)\Bigg[1 + 10\left[\langle {f_1}^2\rangle\left(\frac{A_1}{a}\right)^2 - 2\langle f_1 f_2\rangle\left(\frac{A_1}{a}\right)\left(\frac{A_1}{a}\right) + \langle f_2^2\rangle\left(\frac{A_1}{a}\right)^2\right] + \\ +20\Bigg[\langle {f_1}^3\rangle\left(\frac{A_1}{a}\right)^3 - 3\langle {f_1}^2 f_2\rangle\left(\frac{A_1}{a}\right)^2\left(\frac{A_1}{a}\right) + \end{aligned} \tag{2.16}$$

$$+3\,\langle f_1 {f_2}^2\rangle\left(\frac{A_1}{a}\right)\left(\frac{A_1}{a}\right)^2 - \langle {f_2}^3\rangle\left(\frac{A_1}{a}\right)^3\Bigg]\Bigg] \tag{2.17}$$

The finite conductivity and thermal correction to the force between a spherical disc and a flat plates[14] in the asymptotic limits $\frac{T}{T_{eff}} \ll 1$ as

$$\begin{aligned} F^{C,T}(d) \;\approx\; F(d)\Bigg[1 + \frac{45\zeta_R(3)}{\pi^3}\left(\frac{T}{T_{eff}}\right)^3 - \left(\frac{T}{T_{eff}}\right)^4 \\ -4\frac{\delta_0}{a}\left[1 - 4\frac{45\zeta_R(3)}{2\pi^3}\left(\frac{T}{T_{eff}}\right)^3 + \left(\frac{T}{T_{eff}}\right)^4\right]\Bigg] \end{aligned} \tag{2.18}$$

and for $\frac{T}{T_{eff}} \gg 1$

$$F^{C,T}(d) \approx -\frac{\zeta_R(3)}{4a^2} R k_B T \left(1 - 2\frac{\delta_0}{a}\right) \tag{2.19}$$

where ζ_R is the Riemann zeta function. The roughness correction[15] is given as

$$\begin{aligned} F^R(a) \approx F(a) \Bigg[1 + 6 \Bigg[\langle {f_1}^2 \rangle \left(\frac{A_1}{a}\right)^2 - 2\langle f_1 f_2 \rangle \left(\frac{A_1}{a}\right)\left(\frac{A_1}{a}\right) + \langle f_2^2 \rangle \left(\frac{A_1}{a}\right)^2 \Bigg] + \\ +10 \Bigg[\langle {f_1}^3 \rangle \left(\frac{A_1}{a}\right)^3 - 3\langle {f_1}^2 f_2 \rangle \left(\frac{A_1}{a}\right)^2 \left(\frac{A_1}{a}\right) + \qquad (2.20) \\ +3 \langle f_1 {f_2}^2 \rangle \left(\frac{A_1}{a}\right)\left(\frac{A_1}{a}\right)^2 - \langle {f_2}^3 \rangle \left(\frac{A_1}{a}\right)^3 \Bigg] \Bigg] \qquad (2.21) \end{aligned}$$

2.1.2 Experimental Tests

The earliest experiment to measure Casimir Force was done by Sparnaay[16]. He used a spring balance with a sensitivity of 0.1×10^{-3} dynes. Three sets of parallel plates, Al-Al, Cr-Cr and Cr-Steel, were used. In order to neutralize any electrostatic potential present in the plates, the plates were brought to contact. In spite of using several cleaning procedures, several dust particles 2-3 μm were present. The parallelism was achieved manually. When the experiment was done, Cr-Cr and Cr-Steel plates led to attractive force, while Al-Al led to repulsive force. The anomalous repulsive force was attributed to the dust particles present in the plates. Though the result was not conclusive, Sparnaay concluded that the experiment did not contradict the presence of Casimir force.

A significant advancement in the measuring procedure was done by Van Bockland and Overbeek[17]. In order to overcome the difficulty in keeping the plates in a parallel plate configuration parallel, they used spherical lens and flat plate geometry. The lens and the flat plate were coated with 100±5 nm or 50±5 nm of Cr. A constant potential difference of 20 mV was present. In order to neutralize the electrostatic

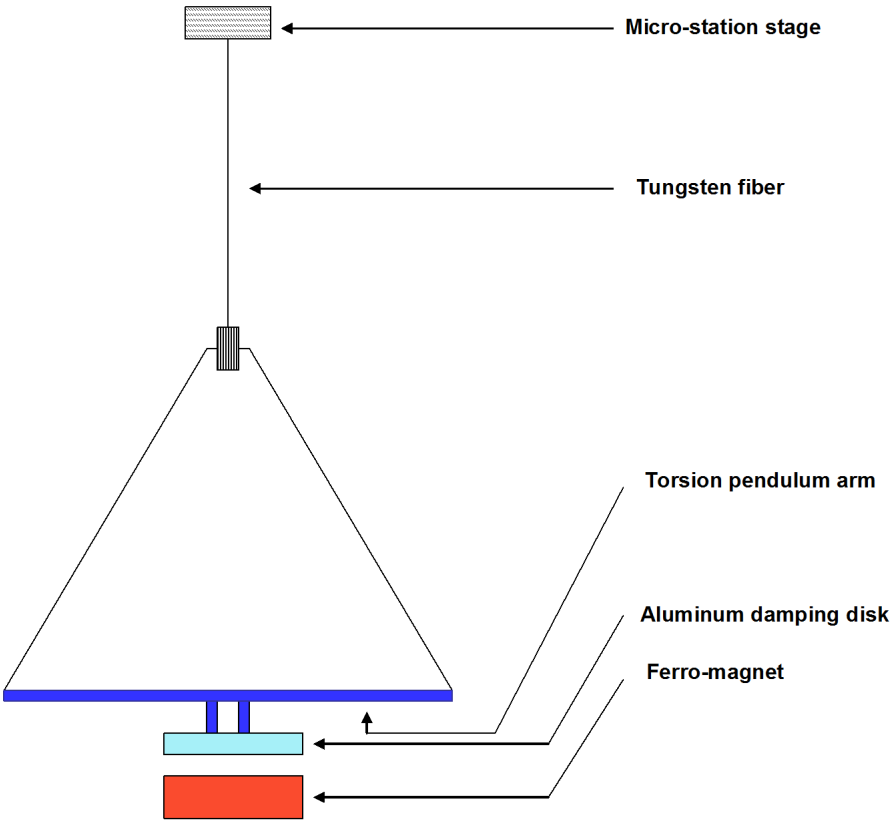

Figure 2.1: Schematic side view of the torsion pendulum apparatus

effects, the experiment was carried out in the presence of compensating voltage. The distance between the lens and plate was found by measuring the capacitance of the system. This experiment confirmed the presence of Casimir force with an accuracy of 50%.

The above two experiments were the earliest landmark experiments which determined the existence of Casimir force unambigously. The first experiment which measured Casimir force with high precision was done by Lamoreaux[18]. He used a high precision torsion pendulum to measure the Casimir force between a lens and flat plate. A schematic view of the apparatus is shown in Fig.(2.1) and Fig.(2.2). The flat plate was 2.54 cm diameter, 0.5 cm thick quartz optical flat, and the spher-

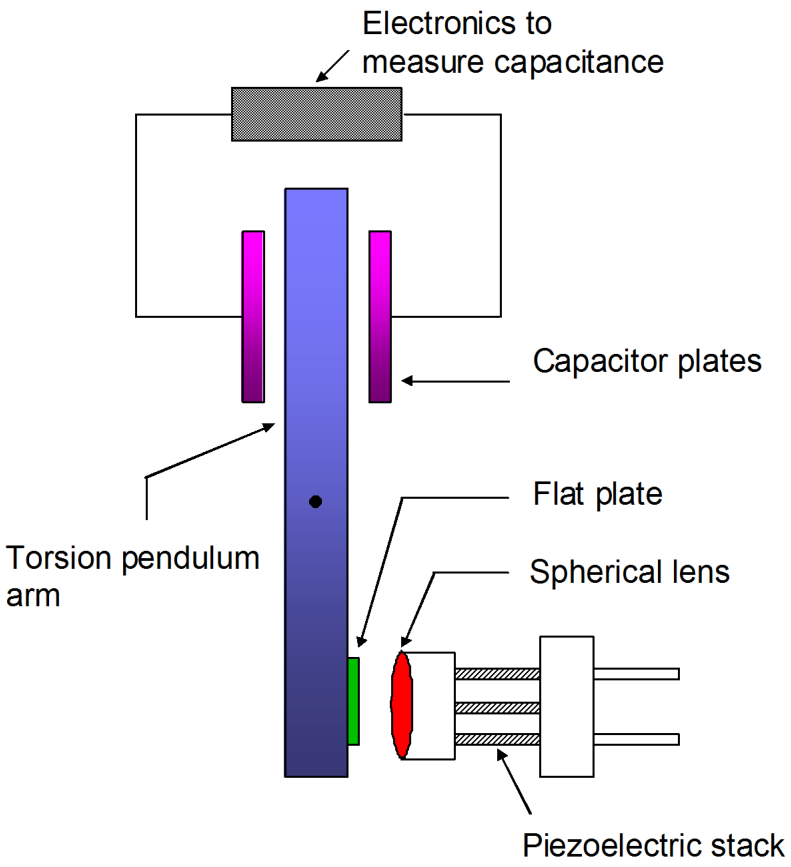

Figure 2.2: Schematic top view of the torsion pendulum apparatus

ical lens was 4 cm diameter with a radius of curvature of 11.3 ± 0.1 cm. Each plate was coated with a layer of 0.5 μm Cu, and 0.5 μm thick layer of Au just on the faces of plate and lens that will be facing each other. The flat plate was mounted on one arm of the torsion pendulum with the lens mounted on a piezoelectric stack translators. The other arm of the pendulum is between two parallel plate capacitor which form the compensator plates. The arms are suspended by tungsten fiber 66 cm long and 76 μm diameter with a torsion constant of $\alpha = 4.8$ dyn/rad. The pendulum was in a vacuum maintained at 10^{-4} torr. The force between the flat plate and the lens is measured by the voltage that is required between the compensator plates, to keep the torsion angle fixed. The sensitivity for this assembly is 48 mV/μm where 1 μm $\sim 2 \times 10^{-5}$ rad. Sixteen data points were taken using this assembly in the range of $0.6 - 6$ μm and the result showed the existence of Casimir force to an accuracy of 5%.

In the following year in 1998, Mohideen et.al.[19], made another precision measurement of Casimir force between sphere and flat using an Atomic Force Microscope (AFM). A schematic view of the apparatus is shown in Fig.(2.3). The sphere was made of Polystyrene and was of diameter 200 ± 4 μm. It was mounted on a cantilever of length 300 μm. The flat plate was a 1.25 cm optically polished saphire disk. Initially, the sphere, cantilever and the saphire disk were coated with 300 nm of Al and then they were coated with less than 20 nm layer of 60% Au/40% Pd. The diameter of the sphere after coating, was measured using an SEM to be 196 μm. The average roughness amplitude measured using an AFM to be 35 nm. The force between the sphere and the flat plate was measure for a total of 256 different distance of separation(data points) in the range $100 - 900$ nm. For each data point 26 scans were done at different regions on the plate. When the temperature, finite conductivity and roughness corrections were taken into account, the percentage difference between theory and experiment was found to be 1%.

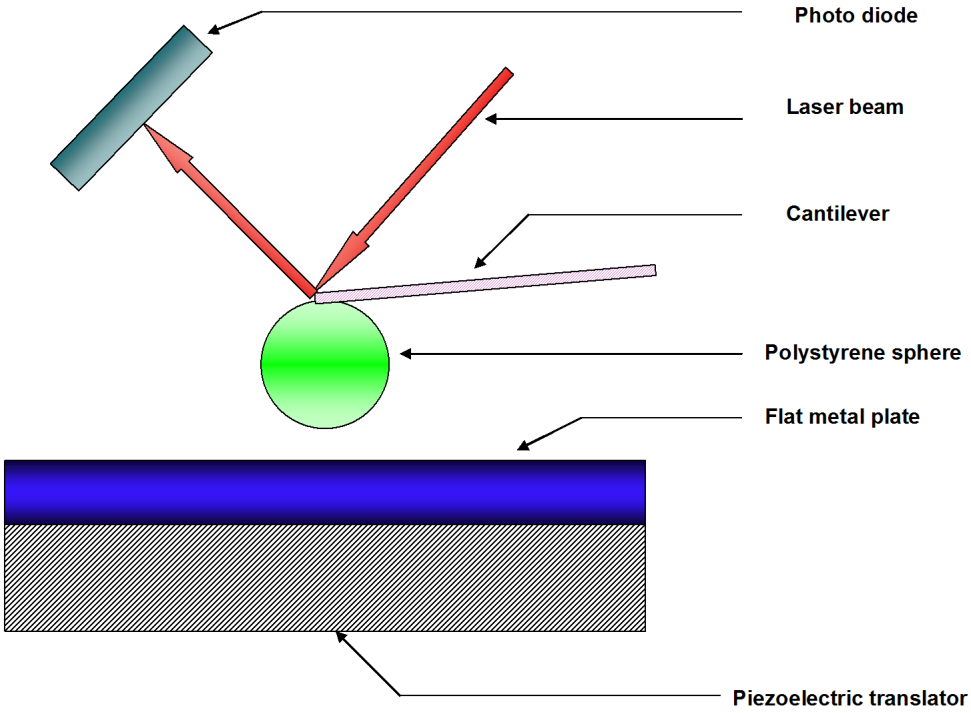

Figure 2.3: Schematic view of the AFM apparatus

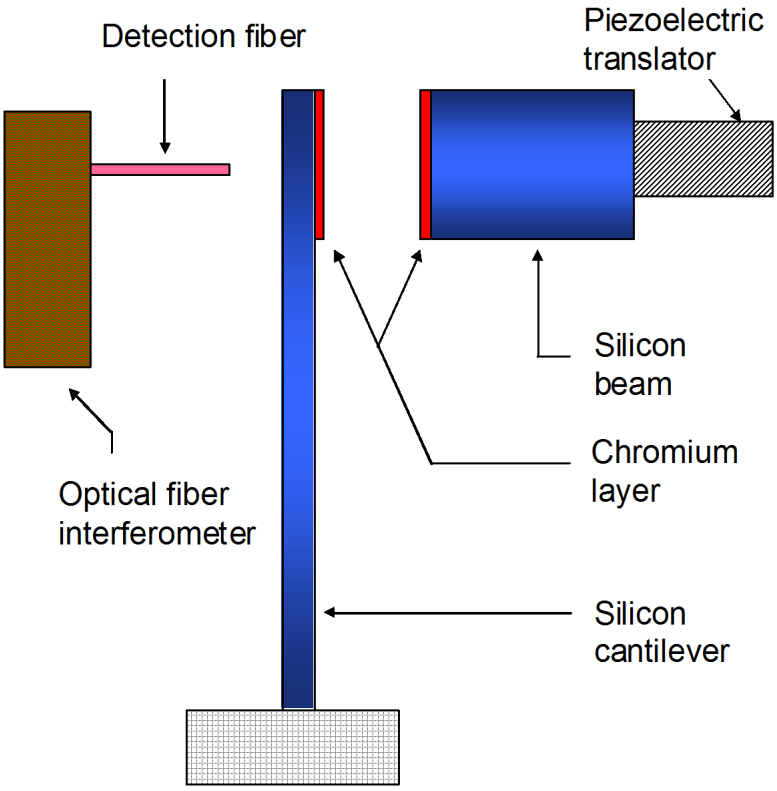

Figure 2.4: Schematic view of the experiment to measure the Casimir force between two parallel plates

Precision measurement for the case of parallel plate geometry, was done by Bressi.et al.[20] by measuring the frequency shift in the torsion mode of a cantilever. A schematic view of the apparatus is shown in Fig.(2.4). A rectangular cross-section silicon cantilever of dimensions 1.9 cm $\times$ 1.2 mm $\times$ 47 μm covered with 50 nm Cr layer, was mounted on a copper base. This surface formed one of the plates of the parallel plate capacitor. The other was mounted on the piezoelectric transducer. The frequency of the resonator was measured by fiber-optic interferometer. The lowest torsional mode frequency (free vibrations) was $\nu_0 = 138.275$ Hz. Dust in the plates were removed to the level of 0.5 μm. The parallel alignment was done first coarsely by an SEM to an accuracy of 1μm and then fine tuned by measuring the capacitance to an accuracy of angular deviation $\sim 3 \times 10^{-5}$ rad. The Casimir force was measured by finding the shift in the frequency of the torsion mode. 21 distances of separation (data points) were taken in the range 0.5-3 μm and the final result of measured Casimir force compared with theory at an accuracy of 15%. Though the precision is much less than that achieved by Mohideen.et.al., it should be noted that the geometry considered here is completely different, that of parallel plates, and it is the highest precision achieved for this particular geometry.

2.2 Static Casimir Effect Stability

2.2.1 Polarization Effects and Ferro-electricity

Consider a dielectric sphere of radius R in a vacuum[21] subject to an external electric field $\mathbf{E}$. The sphere will exhibit a total electric dipole moment $\mathbf{p}$. The total electric field outside the sphere is thereby

$$\mathbf{E}_o = \mathbf{E} + \left[\frac{3\mathbf{rr} - r^2\mathbf{1}}{r^5}\right] \cdot \mathbf{p} \quad \text{for} \quad |\mathbf{r}| > R. \tag{2.22}$$

Inside the dielectric sphere, the electric field is uniform in space; i.e.

$$\mathbf{E}_i = \mathbf{E} - \frac{\mathbf{p}}{R^3} = \mathbf{E} - \frac{4\pi\mathbf{P}}{3} \quad \text{for} \quad |\mathbf{r}| < R. \tag{2.23}$$

With N molecules, the electric dipole moment per unit volume $\mathbf{P}$ inside the dielectric obeys

$$\mathbf{p} = \left(\frac{4\pi R^3}{3}\right)\mathbf{P} = N\alpha\mathbf{E}, \tag{2.24}$$

wherein α is the molecular polarizability response to an external electric field $\mathbf{E}$. Inside the dielectric sphere,

$$\mathbf{D} = \varepsilon\mathbf{E_i} = \mathbf{E_i} + 4\pi\mathbf{P} \quad \text{for} \quad |\mathbf{r}| < R. \tag{2.25}$$

From Eqs.(2.23), (2.24) and Eqs.(2.25), and with $v = (4\pi R^3/3N)$ as the volume per molecule, it follows that

$$\left(\frac{4\pi}{3}\right)\mathbf{P} = \left[\frac{\varepsilon - 1}{\varepsilon + 2}\right]\mathbf{E} = \left(\frac{4\pi\alpha}{3v}\right)\mathbf{E}. \tag{2.26}$$

Thus, the material susceptibility χ obeys

$$\begin{aligned} \varepsilon &= 1 + 4\pi\chi, \\ \chi &= \frac{3\alpha}{3v - 4\pi\alpha}\ . \end{aligned} \tag{2.27}$$

Let us now consider what happens when a finite frequency electric field is applied to the dielectric sphere.

If the molecular polarizability as a function of complex frequency ζ in the upper half complex plane has a single resonance form,

$$\alpha \to \alpha(\zeta) = \left[\frac{\Omega_\infty^2}{\Omega_\infty^2 - \zeta^2}\right]\alpha, \tag{2.28}$$

then the susceptibility

$$\chi \to \chi(\zeta) = \frac{3\alpha(\zeta)}{3v - 4\pi\alpha(\zeta)} \tag{2.29}$$

also has a single resonance form

$$\chi(\zeta) = \left[\frac{\Omega_0^2}{\Omega_0^2 - \zeta^2}\right]\chi, \tag{2.30}$$

but with a down shifted frequency $\Omega_0 < \Omega_\infty$. In detail,

$$\Omega_0^2 = \Omega_\infty^2 \left(1 - \frac{4\pi\alpha}{3v}\right). \tag{2.31}$$

The dielectric sphere is stable for a real frequency Ω_0

$$\Omega_0^2 > 0 \quad \Rightarrow \quad \alpha < (3v/4\pi) \;\; \text{(stable)}. \tag{2.32}$$

and unstable for an imaginary frequency $\Omega_0 = -i\Gamma_0$, i.e. $\Omega_0^2 = -\Gamma_0^2 < 0$. Here Γ_0 is the transition rate per unit time for the sphere to shift out of the unstable phase into a stable phase. That the static susceptibility

$$\chi = \frac{3\alpha}{3v - 4\pi\alpha} \tag{2.33}$$

diverges at the point for which the dielectric sphere becomes unstable, strongly suggests that the stable ordered phase will be ferroelectric with a remnant dipole moment

$$\lim_{\mathbf{E}\to 0} \mathbf{P} = \mathbf{P}_0 \neq 0 \quad \text{(stable ordered phase)}. \tag{2.34}$$

Since the free energy F of an oscillator depends on the frequency Ω,

$$F(\Omega, T) = k_B T \ln\left[2\sinh\left(\frac{\hbar\Omega}{2k_B T}\right)\right], \tag{2.35}$$

a giant Lamb shift from the unperturbed oscillator frequency Ω_∞ to the interacting frequency Ω_0 yields a free energy change

$$\Delta F = \int_{\Omega_\infty}^{\Omega_0} \frac{\partial F(\Omega, T)}{\partial \Omega} d\Omega,$$
$$\Delta F = -\frac{\hbar}{2} \int_{\Omega_0}^{\Omega_\infty} \coth\left(\frac{\hbar\Omega}{2k_B T}\right) d\Omega. \tag{2.36}$$

It is convenient to sum the contributions to ΔF employing Matsubara frequencies $\{\omega_n\}$,

$$\omega_n = \frac{2\pi n k_B T}{\hbar}, \qquad n = 0, \pm 1, \pm 2, \cdots,$$
$$\coth\left(\frac{\hbar\Omega}{2k_B T}\right) = \frac{2k_B T}{\hbar} \sum_{n=-\infty}^{\infty} \left[\frac{\Omega}{\omega_n^2 + \Omega^2}\right]. \tag{2.37}$$

Eqs.(2.36) and (2.37) imply

$$\Delta F = \frac{k_B T}{2} \sum_{n=-\infty}^{\infty} \ln\left[1 + \frac{\Omega_0^2 - \Omega_\infty^2}{\omega_n^2 + \Omega_\infty^2}\right]. \tag{2.38}$$

In the Matsubara frequency summation of Eq.(2.38), the zero frequency contribution is what would ave been obtained if the oscillator were classical, i.e. classical oscillator fluctuations produce

$$\Delta F_{\text{classical}} = \frac{k_B T}{2} \ln\left(\frac{\Omega_0^2}{\Omega_\infty^2}\right). \tag{2.39}$$

The rest of the summation describes additional quantum oscillator fluctuations. Note that the classical contribution to the Casimir free energy change diverges as Ω_0 approaches zero. This constitutes the Casimir effect signature of a phase transition instability.

2.2.2 General Theory

From Maxwell's equations[21], we know that the electric field in the presence of a current density $\mathbf{J}$ and charge density ρ obeys

$$\left[\frac{1}{c^2}\left(\frac{\partial}{\partial t}\right)^2 - \Delta\right]\mathbf{E} = -4\pi\left[\frac{1}{c^2}\frac{\partial \mathbf{J}}{\partial t} + \mathbf{grad}\rho\right] \tag{2.40}$$

When charge is locally conserved,

$$\frac{\partial \rho}{\partial t} + div\mathbf{J} = 0, \tag{2.41}$$

there exists a polarization $\mathbf{P}$ such that

$$\rho = -div\mathbf{P} \quad \text{and} \quad \mathbf{J} = \frac{\partial \mathbf{P}}{\partial t}\ . \tag{2.42}$$

The electric field now obeys

$$\left[\frac{1}{c^2}\left(\frac{\partial}{\partial t}\right)^2 - \Delta\right]\mathbf{E} = 4\pi\left[\mathbf{grad}\ div\mathbf{P} - \frac{1}{c^2}\frac{\partial^2 \mathbf{P}}{\partial t^2}\right]. \tag{2.43}$$

The solution to Eq.(2.43) involves the retarded $Im\zeta > 0$ electromagnetic propagator

$$\mathsf{G}_0\left(\mathbf{r},\zeta\right) = \left[\mathbf{grad}\ \mathbf{grad} + \left(\frac{\zeta}{c}\right)^2 \mathsf{1}\right]\frac{e^{i\zeta r/c}}{r}\ . \tag{2.44}$$

The solution is

$$\mathbf{E}(\mathbf{r},t) = \mathbf{E}_{in}(\mathbf{r},t) + \int \mathsf{G}_0\left(\mathbf{r}-\mathbf{r}',\zeta = i\frac{\partial}{\partial t}\right)\cdot \mathbf{P}(\mathbf{r}',t)d^3\mathbf{r}' \tag{2.45}$$

wherein the incoming electromagnetic field $\mathbf{E_{in}}$ obeys the wave equation

$$\left[\frac{1}{c^2}\left(\frac{\partial}{\partial t}\right)^2 - \Delta\right]\mathbf{E}_{in} = 0 \tag{2.46}$$

The meaning of the parameter ζ becomes evident when we consider the retarded polarization response of matter to a local electric field,

$$\begin{aligned}
\mathbf{P}(\mathbf{r},t) &= \int_0^\infty \int \mathsf{K}(\mathbf{r},\mathbf{r}',s)\cdot\mathbf{E}(\mathbf{r}',t-s)d^3\mathbf{r}'ds,\\
\mathbf{P}(\mathbf{r},t) &= \int_0^\infty \int \mathsf{K}(\mathbf{r},\mathbf{r}',s)\cdot e^{-s(\partial/\partial t)}\mathbf{E}(\mathbf{r}',t)d^3\mathbf{r}'ds,\\
\mathbf{P}(\mathbf{r},t) &= \int \chi\left(\mathbf{r},\mathbf{r}',\zeta = i\frac{\partial}{\partial t}\right)\cdot\mathbf{E}(\mathbf{r}',t)d^3\mathbf{r}',
\end{aligned} \tag{2.47}$$

wherein

$$\chi(\mathbf{r},\mathbf{r}',\zeta) = \int_0^\infty \mathsf{K}(\mathbf{r},\mathbf{r}',s)e^{i\zeta s}ds. \tag{2.48}$$

The electromagnetic scattering Eqs.(2.45) and (2.45) at fixed complex frequency, $\mathbf{E}(\mathbf{r},t) = \Re e\{\mathbf{E}(\mathbf{r};\zeta)e^{-i\zeta t}\}$ then have the form

$$\begin{aligned}
\mathbf{E}(\mathbf{r};\zeta) &= \mathbf{E}_{in}(\mathbf{r};\zeta) +\\
\int\int \mathsf{G}_0(\mathbf{r}-\mathbf{r}',\zeta)\cdot\chi(\mathbf{r}',\mathbf{r}'',\zeta)\cdot\mathbf{E}(\mathbf{r}'';\zeta)d^3\mathbf{r}'d^3\mathbf{r}''
\end{aligned} \tag{2.49}$$

The Fredholm determinant of the scattering integral Eq.(2.49) defines the Jost function

$$\mathcal{F}(-\zeta) = \det\left[1 - \mathsf{G}_0(\zeta)\chi(\zeta)\right]. \tag{2.50}$$

In terms of the spectrum of eigen values eigenvalues $\{\eta_\nu(\zeta)\}$ of the integral operator $\mathsf{G}_0(\zeta)\chi(\zeta)$,

$$\mathsf{G}_0(\zeta)\chi(\zeta)\mathbf{E}_\nu = \eta_\nu(\zeta)\mathbf{E}_\nu = [1 - \mathcal{F}_\nu(-\zeta)]\mathbf{E}_\nu, \tag{2.51}$$

one finds

$$\mathcal{F}(-\zeta) = \prod_{\nu} [1 - \eta_{\nu}(\zeta)] = \prod_{\nu} \mathcal{F}_{\nu}(-\zeta). \tag{2.52}$$

From scattering theory, it is known that the set of Jost functions $\{\mathcal{F}_{\nu}(\pm\zeta)\}$ are related to the set of complex scattering phase shifts $\{\Delta_{\nu}(\zeta)\}$ accordimg to

$$\exp\left(2i\Delta_{\nu}(\zeta)\right) = \frac{\mathcal{F}_{\nu}(\zeta)}{\mathcal{F}_{\nu}(-\zeta)}. \tag{2.53}$$

The set of phase shifts in turn is related to the change in number of the photon states $\mathcal{N}(\omega)$ in the range between zero frequency and frequency ω. To understand this result we employ Levinson's theorem[22, 23] relating $\mathcal{N}(\omega)$ to the Wigner delay times $\{\tau_{\nu}(\omega)\}$; i.e.

$$\begin{aligned} \tau_{\nu}(\omega) &= \frac{d\{\Re e\Delta(\omega + i0^{+})\}}{d\omega} \ , \\ \frac{d\mathcal{N}(\omega)}{d\omega} &= \frac{1}{\pi}\sum_{\nu} \tau_{\nu}(\omega), \end{aligned} \tag{2.54}$$

yielding

$$\mathcal{N}(\omega) = \frac{1}{\pi}\sum_{\nu} \Re e\Delta(\omega + i0^{+}). \tag{2.55}$$

A change in the number of frequency modes leads to a change in the free energy according to the rules

$$
\begin{aligned}
f(\omega,T) &= -k_BT\ln\sum_{n=-\infty}^{\infty} e^{-(n+1/2)\hbar\omega/k_BT},\\
f(\omega,T) &= k_BT\ln\left[2\sinh\left(\frac{\hbar\omega}{2k_BT}\right)\right],\\
\Delta F &= \int_0^\infty f\left(\omega,T\right)d\mathcal{N}(\omega),\\
\Delta F &= -\int_0^\infty \mathcal{N}(\omega)\frac{\partial f(\omega,T)}{\partial\omega}d\omega,\\
\Delta F &= -\frac{\hbar}{2}\int_0^\infty \mathcal{N}(\omega)\coth\left(\frac{\hbar\omega}{2k_BT}\right)d\omega.\\
\Delta F &= -k_BT\sum_{n=-\infty}^{\infty}\int_0^\infty \frac{\omega\mathcal{N}(\omega)d\omega}{\omega^2+\omega_n^2}.
\end{aligned}
\tag{2.56}
$$

wherein Eq.(2.37) has been invoked. In terms of the phase shifts Eqs.(2.55) and (2.56) yield

$$
\Delta F = -\frac{k_BT}{\pi}\sum_{\nu}\sum_{n=-\infty}^{+\infty}\int_0^\infty \frac{\omega\Re e\Delta_\nu(\omega+i0^+)}{\omega^2+\omega_n^2}d\omega, \tag{2.57}
$$

or in terms of the Jost functions

$$
\begin{aligned}
\Delta F = -\frac{k_BT}{\pi}\sum_{\nu}\sum_{n=-\infty}^{+\infty}\times\\
\int_0^\infty \frac{\omega\Im m\ln\mathcal{F}_\nu(-\omega+i0^+)}{\omega^2+\omega_n^2}d\omega.
\end{aligned}
\tag{2.58}
$$

Employing the dispersion relation

$$
\frac{2}{\pi}\int_0^\infty \frac{\omega\Im m\ln\mathcal{F}_\nu(-\omega+i0^+)}{\omega^2-\zeta^2}d\omega = \ln\mathcal{F}_\nu(-\zeta), \tag{2.59}
$$

together with Eqs.(2.52) and (2.58) yields

$$\Delta F = -\frac{k_B T}{2} \sum_{\nu} \sum_{n=-\infty}^{+\infty} \ln \mathcal{F}_{\nu}(-i|\omega_n|),$$
$$\Delta F = -\frac{k_B T}{2} \sum_{\nu} \sum_{n=-\infty}^{+\infty} \ln \left[1 - \eta_{\nu}(i|\omega_n|)\right],$$
$$\Delta F = -\frac{k_B T}{2} \sum_{n=-\infty}^{+\infty} \ln \mathcal{F}(-i|\omega_n|). \tag{2.60}$$

In terms of the Fredholm determinant Eq.(2.50),

$$\Delta F = -\frac{k_B T}{2} \sum_{n=-\infty}^{\infty} \ln \det \left[1 - \mathsf{G}_0(i|\omega_n|)\chi(i|\omega_n|)\right],$$
$$\Delta F = -\frac{k_B T}{2} \sum_{n=-\infty}^{\infty} \mathrm{Tr} \ln \left[1 - \mathsf{G}_0(i|\omega_n|)\chi(i|\omega_n|)\right]. \tag{2.61}$$

The free energy in Eq.(2.61) can be written in terms of the eigenvalues $\{\eta_{\nu}(\zeta)\}$ of the integral operator $\mathsf{G}_0(\zeta)\chi(\zeta)$ according to

$$\Delta F = -\frac{k_B T}{2} \sum_{n=-\infty}^{\infty} \sum_{\nu} \ln \left[1 - \eta_{\nu}(i|\omega_n|)\right]. \tag{2.62}$$

In Eq.(2.62), the free energy is stable if for all n and ν we have $\eta_{\nu}(i|\omega_n|) < 1$. The free energy is unstable if for some n and ν we have $\eta_{\nu}(i|\omega_n|) > 1$. If one writes the Jost function in terms of the spectrum of eigenvalues $\{\eta_{\nu}(\zeta)\}$, as in equation (2.52), one sees that the the roots of the Jost function are precisely the unit magnitudes of one or more eigenvalues $\{\eta_{\nu}\}$. If one solves $\eta_{\nu}(\zeta) = 1$ for $\zeta = i\gamma_{\nu}$, then γ_{ν} represents the transition rate per unit time for an unstable phase in channel ν to move into a stable ordered phase[24, 25, 26, 27].

2.2.3 Application to Bulk Matter

For a bulk translation invariant system[21], Eq.(2.44) and (2.48) may be Fourier transformed into

$$\begin{aligned}
\mathsf{G}_0(\mathbf{r},\zeta) &= \int \mathsf{G}_{\mathbf{k}}(\zeta) e^{i\mathbf{k}\cdot\mathbf{r}} \frac{d^3\mathbf{k}}{(2\pi)^3}, \\
\mathsf{G}_{\mathbf{k}}(\zeta) &= 4\pi \left[\frac{\zeta^2 \mathbf{1} - c^2 \mathbf{k}\mathbf{k}}{c^2 k^2 - \zeta^2} \right], \\
\chi(\mathbf{r}-\mathbf{r}',\zeta) &= \int \chi_{\mathbf{k}}(\zeta) e^{i\mathbf{k}\cdot(\mathbf{r}-\mathbf{r}')} \frac{d^3\mathbf{k}}{(2\pi)^3}.
\end{aligned} \tag{2.63}$$

The eigenvalues in Eq.(2.51) involve plane wave eigenfunctions $\mathbf{E}_{\mathbf{k}}(\mathbf{r}) = \mathbf{E}_{\mathbf{k}} e^{i\mathbf{k}\cdot\mathbf{r}}$ yielding the three by three matrix eigenvalue problem

$$\mathsf{G}_{\mathbf{k}}(\zeta) \cdot \chi_{\mathbf{k}}(\zeta) \cdot \mathbf{E}_{\mathbf{k}\lambda} = \eta_{\mathbf{k}\lambda}(\zeta) \mathbf{E}_{\mathbf{k}\lambda} \quad (\lambda = 1,2,3). \tag{2.64}$$

If the susceptibility has longitudinal and transverse parts accordung to

$$\chi_{\mathbf{k}}(\zeta) = \chi_{\mathbf{k}L}(\zeta) \frac{\mathbf{k}\mathbf{k}}{k^2} + \chi_{\mathbf{k}T}(\zeta) \left[\mathbf{1} - \frac{\mathbf{k}\mathbf{k}}{k^2} \right], \tag{2.65}$$

then the eigenvalues obey

$$\begin{aligned}
\eta_{\mathbf{k}T}(\zeta) &= \frac{4\pi\zeta^2 \chi_{\mathbf{k}T}(\zeta)}{c^2 k^2 - \zeta^2} \qquad (\lambda = 1,2), \\
\eta_{\mathbf{k}L}(\zeta) &= -4\pi \chi_{\mathbf{k}L}(\zeta) \qquad (\lambda = 3).
\end{aligned} \tag{2.66}$$

The Casimir free energy per unit volume Δf follows from Eqs.(2.62) and (2.66); it is

$$\Delta f = -\frac{k_B T}{2} \sum_{\lambda=1,2,3} \left\{ \sum_{n=-\infty}^{\infty} \int \ln\left[1 - \eta_{\mathbf{k}\lambda}(i|\omega_n|)\right] \frac{d^3\mathbf{k}}{(2\pi)^3} \right\}. \tag{2.67}$$

which contains one longitudinal and two transverse parts

$$\begin{aligned} \Delta f &= \Delta f_L + \Delta f_T \ , \\ \Delta f_L &= -\frac{k_B T}{2} \sum_{n=-\infty}^{\infty} \int \ln\left[1 - \eta_{\mathbf{k}L}(i|\omega_n|)\right] \frac{d^3\mathbf{k}}{(2\pi)^3} \ , \\ \Delta f_T &= -k_B T \sum_{n=-\infty}^{\infty} \int \ln\left[1 - \eta_{\mathbf{k}T}(i|\omega_n|)\right] \frac{d^3\mathbf{k}}{(2\pi)^3} \ . \end{aligned} \tag{2.68}$$

From Eqs.(2.66) and (2.68), one finds the longitudinal contribution

$$\begin{aligned} \Delta f_L = -\frac{k_B T}{2} \sum_{n=-\infty}^{\infty} \int \ln\left[\varepsilon_{\mathbf{k}L}(i|\omega_n|)\right] \frac{d^3\mathbf{k}}{(2\pi)^3} \ , \\ \varepsilon_{\mathbf{k}L}(\zeta) = 1 + 4\pi\chi_{\mathbf{k}L}(\zeta), \end{aligned} \tag{2.69}$$

and the transverse contribution

$$\begin{aligned} \Delta f_T = -k_B T \sum_{n=-\infty}^{\infty} \\ \int \ln\left[\frac{c^2k^2 + \varepsilon_{\mathbf{k}T}(i|\omega_n|)\omega_n^2}{c^2k^2 + \omega_n^2}\right] \frac{d^3\mathbf{k}}{(2\pi)^3} \ , \\ \varepsilon_{\mathbf{k}T}(\zeta) = 1 + 4\pi\chi_{\mathbf{k}T}(\zeta). \end{aligned} \tag{2.70}$$

The classical contribution to the Casimir free energy comes from the $n = 0$ part of the frequency summation and, in accordance with Eqs.(2.69) and (2.70), only from

the longitudinal part

$$\Delta f_{classical} = -\frac{k_B T}{2} \int \ln \left[\varepsilon(k,T)\right] \frac{d^3\mathbf{k}}{(2\pi)^3} \ , \tag{2.71}$$

wherein $\varepsilon(k,T)$ is the static wave number and temperature dependent dielectric constant. If the dielectric response function for the ferroelectric[28] above the critical temperature $T > T_c$, has a singularity of the form $\varepsilon(0,T) \sim |T - T_c|^{-\gamma}$ as $T \to T_c + 0^+$, then such singularities become manifest in the free energy per unit volume shift of Eq.(2.71). In more detail, one expects near the critical point that

$$\varepsilon(k,T) = \frac{\varepsilon(0,T)}{1 + k^2 \xi(T)^2} \quad \text{as} \quad k \to 0 \tag{2.72}$$

wherein the coherence length obeys $\xi(T) \sim |T - T_c|^{-\nu}$ as $T \to T_c + 0^+$. The critical singularities in the dielectric response $\varepsilon(0,T)$ and coherence length $\xi(T)$ produce a logarithmic shift in the free energy Eq.(2.71) yielding only a weak singularity in the specific heat.

2.3 Ferroelectric Phase Transitions

2.3.1 General Formalism

Let H be a hamiltonian that describes the mesoscopic object at temperature T. Then the partition function of the object is given by

$$Z = \mathrm{Tr}\ \mathrm{e}^{-\beta \mathrm{H}} \tag{2.73}$$

The free energy of the object is given by

$$F = -\frac{1}{\beta} \ln Z \tag{2.74}$$

Let this object interact with photons described by oscillator coordinates P and Q. The coupling between the object and the oscillator is described by a force f. The hamiltonian for the system H' can be written as

$$H' = \frac{1}{2}P^2 + \frac{1}{2}\omega_\infty^2 Q^2 + H - fQ \tag{2.75}$$

The partition function for the system is given by

$$\begin{aligned} Z' &= \int_{-\infty}^{\infty}\int_{-\infty}^{\infty} \mathrm{Tr}\ \mathrm{e}^{-\beta \mathrm{H}'} \frac{\mathrm{dQdP}}{2\pi\hbar} \\ &= \int_{-\infty}^{\infty}\int_{-\infty}^{\infty} \mathrm{Tr}\ \mathrm{e}^{-\beta(\frac{1}{2}\mathrm{P}^2 + \frac{1}{2}\omega_\infty^2 \mathrm{Q}^2 + \mathrm{H} - \mathrm{fQ})} \frac{\mathrm{dQdP}}{2\pi\hbar} \\ &= \frac{1}{\sqrt{2\pi\beta\hbar^2}} \int_{-\infty}^{\infty} \mathrm{Tr}\ \mathrm{e}^{-\beta(\frac{1}{2}\omega_\infty^2 \mathrm{Q}^2 + \mathrm{H} - \mathrm{fQ})} \mathrm{dQ} \end{aligned} \tag{2.76}$$

The free energy of the system is given by

$$F' = \frac{-1}{\beta} \ln Z' \tag{2.77}$$

Using Eqs.(2.74)and (2.77), the shift in free energy of the system due to the interaction is given by

$$F' - F = \frac{-1}{\beta} \ln \left(\frac{Z'}{Z} \right) \tag{2.78}$$

One can rewrite this as

$$e^{-\beta(F'-F)} = \frac{Z'}{Z} \tag{2.79}$$

Using Eqs.(2.73) and (2.76), we have

$$e^{-\beta(F'-F)} = \frac{\frac{1}{\sqrt{2\pi\beta\hbar^2}}\int_{-\infty}^{\infty} \mathrm{Tr}\ \mathrm{e}^{-\beta(\frac{1}{2}\omega_\infty^2 \mathrm{Q}^2+\mathrm{H}-\mathrm{fQ})}\mathrm{dQ}}{\mathrm{Tr}\ \mathrm{e}^{-\beta\mathrm{H}}} \tag{2.80}$$

The right hand side of Eq.(2.80) can be rewritten in the form

$$\begin{aligned} e^{-\beta(F'-F)} &= N\int_{-\infty}^{\infty} e^{-\beta\left(\frac{1}{2}\omega_\infty^2 Q^2-\frac{1}{\beta}\ln\left(\frac{\mathrm{Tr}\ \mathrm{e}^{-\beta(\mathrm{H}-\mathrm{fQ})}}{\mathrm{Tr}\ \mathrm{e}^{-\beta\mathrm{H}}}\right)\right)}\mathrm{dQ} \\ N &= \frac{1}{\sqrt{2\pi\beta\hbar^2}} \end{aligned} \tag{2.81}$$

Comparing the form of the arguments in the exponents of both the sides of the Eq.(2.81), we define free energy as a function of oscillator coordinate to be

$$G\left(Q,\beta\right) = \frac{1}{2}\omega_\infty^2 Q^2 - \frac{1}{\beta}\ln\left(\frac{\mathrm{Tr}\ \mathrm{e}^{-\beta(\mathrm{H}-\mathrm{fQ})}}{\mathrm{Tr}\ \mathrm{e}^{-\beta\mathrm{H}}}\right) \tag{2.82}$$

From this equation, the shifted frequency of the oscillator due to the interaction is given by

$$\lim_{Q\to\ 0}\left(\frac{G\left(Q,\beta\right)}{Q^2}\right) = \frac{\omega_0^2}{2} \tag{2.83}$$

2.3.2 Free Energy Calculations for Spin Zero System

We first start by defining the Hamiltonian that describes the system and find the corresponding eigenvalues.

The Hamiltonian H_0 of a single particle in the system, without interaction is given by the matrix

$$H_0 = \begin{pmatrix} -\Delta & 0 & 0 & 0 \\ 0 & \Delta & 0 & 0 \\ 0 & 0 & \Delta & 0 \\ 0 & 0 & 0 & \Delta \end{pmatrix} \tag{2.84}$$

The Eigenvalues of this hamiltonian are

$$\lambda_1 = -\Delta;\ \lambda_{2,3,4} = +\Delta \tag{2.85}$$

If the particle interacts with the oscillator via electric dipole interaction, then the new hamiltonian is given by

$$H_1 = \begin{pmatrix} -\Delta & -\mu E_x & -\mu E_y & -\mu E_z \\ -\mu E_x & \Delta & 0 & 0 \\ -\mu E_y & 0 & \Delta & 0 \\ -\mu E_z & 0 & 0 & \Delta \end{pmatrix} \tag{2.86}$$

The eigenvalues of this matrix are,

$$\lambda'_{1,2} = +\Delta;\ \lambda'_3 = +\sqrt{\Delta^2 + \mu^2|\mathbf{E}|^{\mathbf{2}}};\ \lambda'_4 = -\sqrt{\Delta^2 + \mu^2|\mathbf{E}|^{\mathbf{2}}} \tag{2.87}$$

The Hamiltonian for the system composed of N identical particles, not interacting among themselves, but interacting with the photons via electric dipole interaction is given by

$$\mathbf{H} = \sum_{i=1}^{N} H_{1i} \tag{2.88}$$

where the index i, denotes the i-th particle.

The energy stored in the electric field can be expressed as

$$\frac{1}{8\pi}\int |\mathbf{E}|^{\mathbf{2}}\mathrm{d}^3\mathbf{r} = \frac{\mathbf{1}}{\mathbf{2}}\omega_{\infty}^{\mathbf{2}}\mathrm{Q}^2 \tag{2.89}$$

Using this relation, the electric field can be expressed as

$$\mathbf{E}(\mathbf{r}) = \sqrt{4\pi}\omega_{\infty}\mathrm{Q}\mathbf{e}(\mathbf{r}) \tag{2.90}$$

If the object is placed in such a way that the filed is concentrated over an effect length of L, then we have the relation,

$$\mathbf{e}(\mathbf{r}) = \frac{\mathbf{n}}{\mathrm{L}^{\frac{3}{2}}} \tag{2.91}$$

Using this relation we have

$$|\mathbf{E}|^{\mathbf{2}} = \frac{1}{\mathrm{L}^3}4\pi\omega_{\infty}^2\mathrm{Q}^2 \tag{2.92}$$

In Sec.(2.3.1) a general formalism describing the free energy shifts due to interaction of a mesoscopic object with the oscillator was developed. The resulting free energy shift was given by the Eq.(2.82).The hamiltonian H in Eq.(2.82) is given the Eq.(2.84) and the hamiltonian $H - fQ$ is given by the Eq.(2.86). Using Eq.(2.85), we have

$$\begin{aligned} \mathrm{Tr}\ \mathrm{e}^{-\beta\mathrm{H}} &= \sum_{i=1}^{4} e^{-\beta\lambda_i} \\ &= e^{\beta\Delta} + 3e^{-\beta\Delta} \end{aligned} \tag{2.93}$$

Using Eqs.(2.87) and (2.92), we have

$$\begin{aligned}
\mathrm{Tr}\ \mathrm{e}^{-\beta(\mathrm{H}-\mathrm{fQ})} &= \sum_{i=1}^{4} e^{-\beta\lambda_i'} \\
&= 2e^{-\beta\Delta} + \\
&\quad 2\cosh\left(\beta\sqrt{\Delta^2 + \frac{1}{L^3}\mu^2 4\pi\omega_\infty^2 Q^2}\right) \\
&= 2e^{-\beta\Delta} + 2\cosh\left(\beta\Delta\sqrt{1 + \frac{4\pi\mu^2\omega_\infty^2 Q^2}{\Delta^2 L^3}}\right)
\end{aligned} \tag{2.94}$$

Using Eqs.(2.93) and (2.94), Eq.(2.82) for the spin zero system under consideration is

$$\begin{aligned}
G_1(Q,\beta) &= \frac{1}{2}\omega_\infty^2 Q^2 - \frac{1}{\beta} \times \\
&\quad \ln\left(\frac{2e^{-\beta\Delta} + 2\cosh\left(\beta\Delta\sqrt{1 + \frac{4\pi\mu^2\omega_\infty^2 Q^2}{\Delta^2 L^3}}\right)}{e^{\beta\Delta} + 3e^{-\beta\Delta}}\right)
\end{aligned} \tag{2.95}$$

The subscript 1, refers to the case when interaction of photons with just one particle is considered. The corresponding free energy shift due to the interaction of photons with N particles is

$$\begin{aligned}
G_N(Q,\beta) &= \frac{1}{2}\omega_\infty^2 Q^2 - N\frac{1}{\beta} \times \\
&\quad \ln\left(\frac{2e^{-\beta\Delta} + 2\cosh\left(\beta\Delta\sqrt{1 + \frac{4\pi\mu^2\omega_\infty^2 Q^2}{\Delta^2 L^3}}\right)}{e^{\beta\Delta} + 3e^{-\beta\Delta}}\right)
\end{aligned} \tag{2.96}$$

Using Eq.(2.83), we have

$$\frac{\omega_0^2}{\omega_\infty^2} = \left[1 - \frac{4\pi N\mu^2}{\Delta L^3}\frac{\sinh(\beta\Delta)}{e^{-\beta\Delta} + \cosh(\beta\Delta)}\right] \tag{2.97}$$

The critical temperature is defined as the one for which the right hand side of the Eq.(2.97) vanishes and starts becoming negative. It is given expression,

$$\frac{\sinh(\beta_c\Delta)}{e^{-\beta_c\Delta} + \cosh(\beta_c\Delta)} = \frac{\Delta L^3}{4\pi N\mu^2} \tag{2.98}$$

The position of the new equilibrium is given by condition

$$\frac{\partial G}{\partial Q} = 0 \tag{2.99}$$

For the sake of brevity, we introduce new parameters $x,\ y,\ \alpha(y)$ and u defined as

$$\begin{aligned} x &= \frac{T}{T_c} \\ y &= \beta_c\Delta \\ \alpha(y) &\equiv \frac{e^{-y} + \cosh y}{\sinh y} \\ u &= \sqrt{1 + \frac{Q_e^2}{Q_0^2}\left(\alpha(y)^2 - 1\right)} \end{aligned} \tag{2.100}$$

where Q_e is the equilibrium oscillator coordinate and Q_0 is the equilibrium oscillator coordinator at temperature $T = 0$. We have the final implicit equation for the

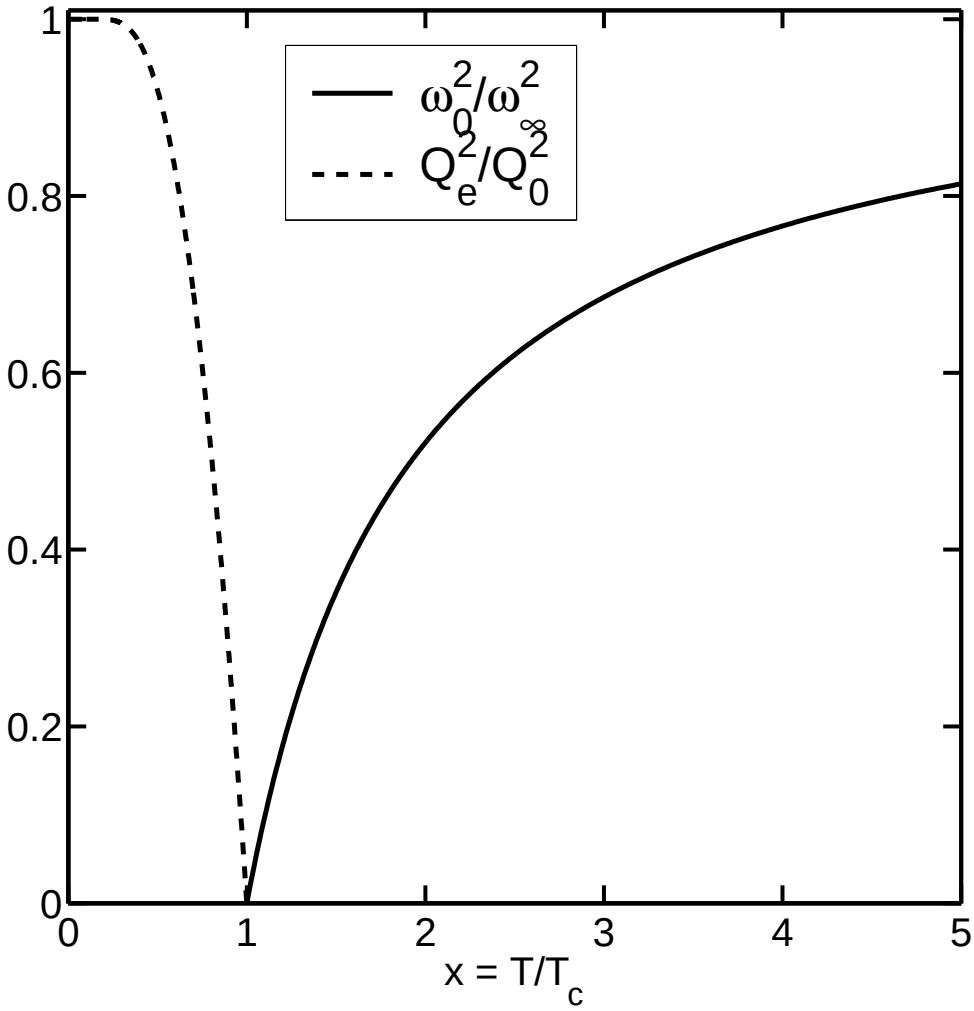

Figure 2.5: Plot of $\frac{\omega_0^2}{\omega_\infty^2}$ and $\frac{Q_e^2}{Q_0^2}$ vs x. Here $y = 0.2$.

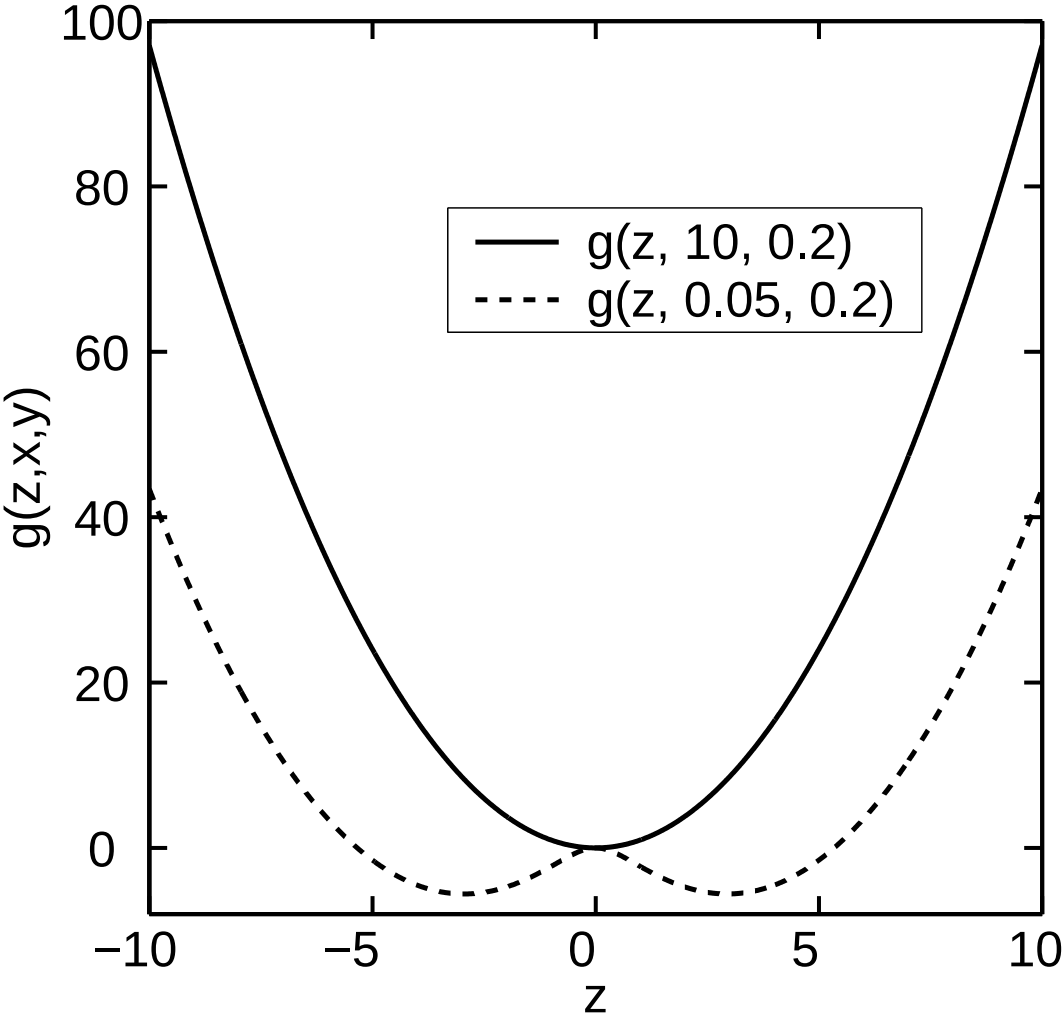

Figure 2.6: Plot of $g(z, x, y)$ vs z where $g(z, x, y) = \frac{G_N}{k_B T}$ and $z = \frac{\omega_\infty Q}{\sqrt{N K_B T}}$. The plot is shown for two values of x. viz. $x = 10$ and $x = 0.05$. Here $y = 0.2$.

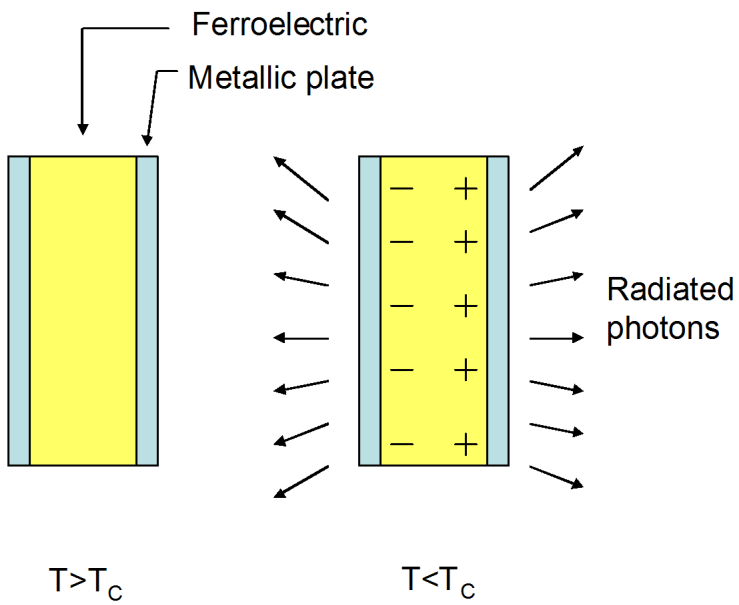

Figure 2.7: Ferroelectric phase transition

equilibrium oscillator as

$$\frac{\sinh\left(\frac{y}{x}u\right)}{e^{\frac{y}{x}} + \cosh\left(\frac{y}{x}u\right)} = u\frac{1}{\alpha(y)} \tag{2.101}$$

where The range of the variable x, is $0 < x < 1$.

The expression in Eq.(2.97) in terms of the dimensionless parameters defined in Eq.(2.100) takes the form

$$\frac{\omega_0^2}{\omega_\infty^2} = \left[1 - \frac{1}{\alpha(y)}\frac{\sinh\left(\frac{y}{x}\right)}{e^{-\frac{y}{x}} + \cosh\left(\frac{y}{x}\right)}\right] \tag{2.102}$$

The range of x here is $x \geq 1$.The plot is shown in Fig.(2.5), for $y = 0.2$.

As can be seen from the plot, when the temperature is lowered (i.e as x decreases) ω_0^2 decreases, and vanishes when $x = 1$. When $x < 1$, a double well emerges in the free energy plot Fig(2.6) and hence a new equilibrium coordinate Q_e emerges and the ferroelectric becomes polarized. As we cool further, the well deepens and radiates out the photons from vacuum as shown in Fig(2.7). The new equilibrium coordinate reaches the value Q_0 when $T = 0$.

Chapter 3

Dynamic Casimir Effect

3.1 History

3.1.1 Theoretical Considerations

One of the earliest effects which deal with production of photons from vacuum, is the prediction of Unruh-Davies-Fulling-Witt Radiation, which states that an accelerating reference frame in vacuum would see thermal radiation of temperature T given by

$$kT = \left(\frac{\hbar}{2\pi}\right)\left(\frac{a}{c}\right) \tag{3.1}$$

an experimental verification of the effect is inaccessible by conventional means of acceleration, because, an acceleration of g = 9.8 ms^{-2} would yield thermal radiations at temperature T = 4$\times$ 10^{-20} K which is extremely faint to detect experimentally. In order to beat this limitation, Yablonovitch suggested[29] the use of optical techniques to mimic the acceleration of a physical mirror. He suggested that by optically exciting a semiconductor slab by laser pulses, one can change the refractive index of the slab n = 3.5 to n = 0 in very short times $\tau \sim 10^{-10}$ s thereby changing the mirror

surface from one face of the slab to the other. This in effect, simulates the motion of the mirror from one face to the other with an acceleration of a $\sim 10^{21}$ ms^{-2}. He calculated the number of photons produced by this effect in the accelerated k-mode to be

$$\langle 0|b_k^\dagger b_k|0\rangle = \sum_{k'} |\beta_{kk'}|^2$$
$$\text{where} \quad \beta_{\mathrm{kk'}} = \delta_{\mathrm{kk'}} \frac{\mathrm{n} - \mathrm{n}_0}{2\sqrt{\mathrm{nn}_0}} \tag{3.2}$$

where $n - n_0$ is the instantaneous change in the refractive index of the slab and $\delta_{kk'}$ is the Kronecker delta.

Later Lambrecht et al.[30] considered the effect on photon generation due to the oscillatory motion of a mirror. First he considered the one dimensional case wherein a single mirror is subjected to a harmonic oscillation

$$x(t) = 2a\cos(\Omega t) \qquad 0 < t < T \tag{3.3}$$

He showed the number of radiated photons to be

$$\frac{N}{T} = \frac{2a^2\Omega^3}{3\pi c^2} \tag{3.4}$$

He then considered the case of two parallel mirrors vibrating with amplitudes a_1 and a_2 but with the same frequency Ω. The number of photons outside the cavity was found to be

$$\frac{N}{T} = \frac{\Omega^3}{3\pi c^3}\left(a_1^2 + a_2^2\right) + \frac{\Omega}{6\pi c^2}\left(\Omega^2 - \frac{\pi^2}{\tau^2}\right)\frac{\sinh(2\rho)(a_1+a_2)^2}{\cosh(2\rho)+\cos(\Omega\tau)} + \frac{\Omega}{6\pi c^2}\left(\Omega^2 - \frac{\pi^2}{\tau^2}\right)\frac{\sinh(2\rho)(a_1-a_2)^2}{\cosh(2\rho)-\cos(\Omega\tau)} \tag{3.5}$$

where, 4ρ is the probability that a photon escapes the cavity after making a round

trip in time 2τ. Resonance occurs when $\Omega = \frac{2n\pi}{\tau}$ which corresponds to the periodic modulation of the cavity length and $\Omega = \frac{(2n+1)\pi}{\tau}$ which corresponds to the oscillation of the cavity as a whole.

The case for photon generation in a three dimensional rectangular cavity is considered by Sasarolli et al.[31], wherein the length of one of the dimensions of the cavity x(t) is modulated. The mode frequency in the cavity is given by

$$\omega_k(t) = \pi c \left[\left(\frac{l}{x(t)} \right)^2 + \left(\frac{m}{y} \right)^2 + \left(\frac{n}{z} \right)^2 \right]^{\frac{1}{2}} \tag{3.6}$$

. The modes inside the cavity are shown to obey the differential equation

$$\frac{d^2}{dt^2} q_k(t) + \omega_k^2(t) q_k(t) = 0 \tag{3.7}$$

and the photons generated is shown to be

$$N_k(\omega) = \frac{|R_{fk}(\omega)|^2}{1 - |R_{fk}(\omega)|^2} = \frac{|R_{bk}(\omega)|^2}{1 - |R_{bk}(\omega)|^2} \tag{3.8}$$

where $R_{fk}$and $\mathrm{R_{bk}}$ are the forward reflection coefficient and backward reflection coefficient respectively. The special case where $\omega(t) = \omega_1$ when $\frac{-\mathrm{T}}{4} < \mathrm{t} < \frac{\mathrm{T}}{4}$ and $\omega(\mathrm{t}) = \omega_2$ when $\frac{\mathrm{T}}{4} < \mathrm{t} < \frac{3\mathrm{T}}{4}$ is also solved exactly.

Dodonov et al.[32], obtain a relation between the period T of the vibration of the cavity wall and the the period T_0 of the cavity mode for resonance as

$$T = \frac{T_0}{2} \left(m + \frac{\phi}{\pi} \right) \tag{3.9}$$

where ϕ is the phase of the mode. Under this condition the number of photons

produced in the cavity is given by

$$\begin{aligned} N &= \sinh^2(\nu) \\ &\equiv \frac{1}{4}\left[\left(\frac{1+|r|}{1-|r|}\right)^{\frac{n}{2}} - \left(\frac{1-|r|}{1+|r|}\right)^{\frac{n}{2}}\right]^2 \end{aligned} \tag{3.10}$$

where $r = R_{bk}$ is the backward reflection coefficient. Asymptotically this can be written as

$$N \approx \frac{1}{4}\exp(2n|r|) \tag{3.11}$$

He then considers effect of vibration of the cavity at frequencies near the resonance condition, on the photon generation rates. When the modes in the cavity vary as

$$\omega(t) = \omega_0\left[1 + 2\epsilon\sin(\Omega t)\right], \quad \text{where} \quad \Omega = 2(\omega_0 + \delta) \tag{3.12}$$

the number of photons generated is given by

$$N = \frac{\sinh^2(\omega_0\epsilon\gamma t)}{\gamma^2}, \quad \text{where} \quad \gamma^2 = 1 - \frac{\delta^2}{(\omega_0\epsilon)^2} \tag{3.13}$$

Hence, photon generation is possible only when $\delta < \epsilon\omega_0$. He also considers the effect of phase fluctuations on photon generation. The fluctuation in phase when $\delta = 0$ can be written as

$$\theta_k = k\theta + \chi_k, \quad \text{where} \quad \theta = \theta_{\text{res}} \equiv \mathrm{m}\pi + \phi \tag{3.14}$$

where χ_k is a purely random variable. The number of photons generated is given by

$$N = \frac{1}{2}\left(\frac{1+|r|}{1-|r|}\right)^n - \frac{1}{2} \tag{3.15}$$

Asymptotically this can be written as

$$N \approx \frac{1}{2}\exp(2n|r|^2) \tag{3.16}$$

Dalvit et al.[33], considered photon generation in various other geometries. For the case of cylindrical cavity with length $L_z(t)$ and radius R, the length $L_z(t)$ is modulated as

$$L_z(t) = L_0(1 + \epsilon \sin(\Omega t)) \tag{3.17}$$

the eigenfrequencies are given by

$$\omega_{n,m,n_z} = \sqrt{\left(\frac{y_{nm}}{R}\right)^2 + \left(\frac{n_z \pi}{L_z}\right)^2} \tag{3.18}$$

where y_{nm} is the $m - th$ root of $J_n'(x)$. The photons in the $\omega_{1,1,1}$ mode grows as

$$N_{1,1,1} \approx \exp\left(\frac{\pi \epsilon t}{\sqrt{1 + 0.343(L_z/R)^2}}\right) \tag{3.19}$$

and the photons in $\omega_{0,1,0}$ mode grows as

$$N_{0,1,0} \approx \exp\left(\frac{4.81 \epsilon t}{R}\right) \tag{3.20}$$

when parametrically excited. The condition for parametric resonance in either case is $\Omega = 2\omega_k$. In the case of a spherical cavity where the radius $a(t)$ is modulated as

$$a(t) = a_0[1 + \epsilon \sin(\Omega t)] \tag{3.21}$$

The eigenfrequencies of the modes are given by

$${\omega_{lk}}^{TE} = \frac{j_{lk}}{a_0}, \quad {\omega_{lk}}^{TM} = \frac{k_{lk}}{a_0} \tag{3.22}$$

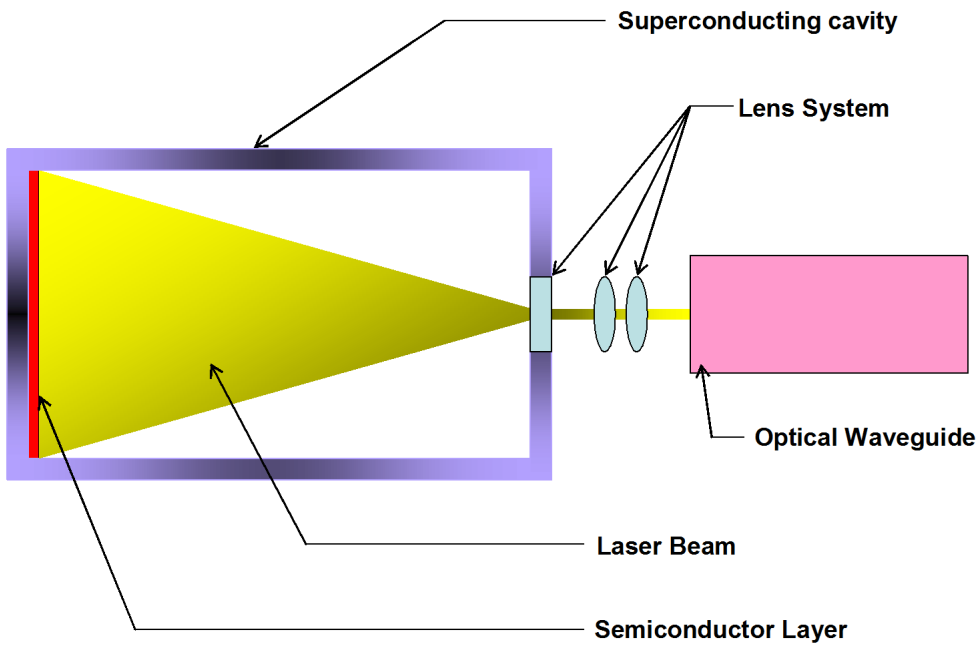

Figure 3.1: Schematic view experimental setup

Under the parametric resonance condition $\Omega = 2\omega_{lk}$, the number of photons in the cavity is given by

$$\begin{aligned} N_{lk} &\approx \exp(2\gamma\epsilon t), \quad \text{where} \\ {\gamma_{lk}}^{TE} &= \frac{{\omega_{lk}}^{TE}}{2}, \quad {\gamma_{lk}}^{TM} = \frac{{\omega_{lk}}^{TM}}{2}\frac{\kappa_{lk}^2 + l(l+1)}{\kappa_{lk}^2 - l(l+1)} \end{aligned} \tag{3.23}$$

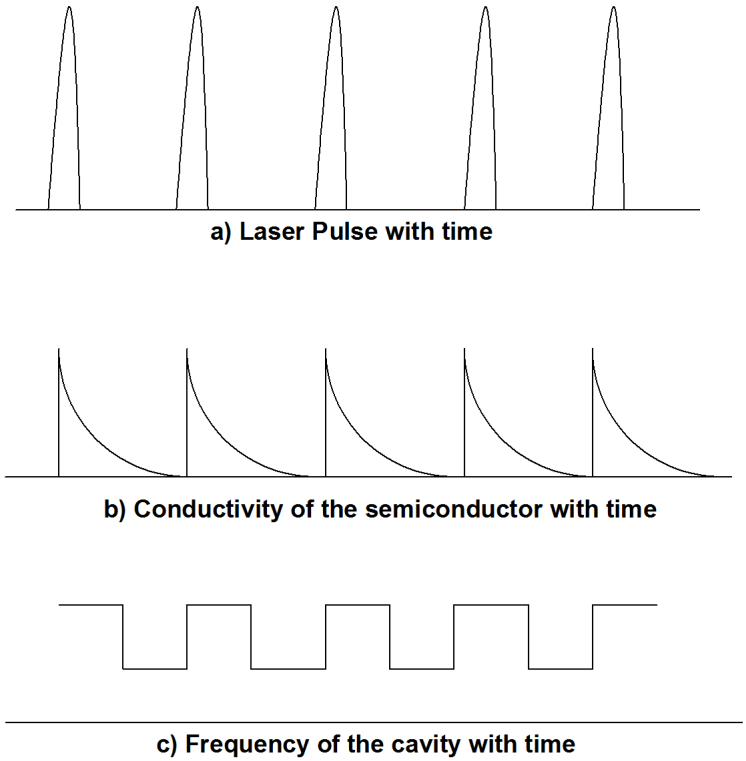

Figure 3.2: Schematic view of the process which changes the cavity frequency

3.1.2 Experimental Difficulties and Recently Proposed Dynamic Casimir Effect Experiment

Mechanical vibrations of the cavity wall at GHz frequencies is not possible due to the enormous power that is required. Since the maximum kinetic energy is $\frac{1}{2}\rho V\omega^2 A^2$, where A is the amplitude of vibration, an estimate for the power required can be made by making a reasonable estimate of the parameters A, ρ and V. If A is $\sim 10^{-3}$ m, if the density is $\sim 10^3$ Kg/m^3, volume of the wall under vibration is $\sim 10^{-9}$ m^3 and $\omega \sim 10^{10}$ Hz, the power is$\sim 10^8$ Watts.

Vibration of the cavity walls by acoustic means using piezoeffect has been suggested[35]. Even using piezoeffect, vibration in the GHz frequency has not been achieved. Another major problem with acoustic vibrations is heating effect. In order to prevent any loss of photons that will be generated in the experiment, the cavity should be high quality factor $\sim 10^{10}$ super conducting cavity. Any heating effect, if not properly removed, might destroy the superconductivity.

In order to circumvent all these problems, a novel experiment using optical means has been suggested. A schematic view of the experimental setup is shown in Fig.(3.1). It consists of a super-conducting Nb microwave cavity, a GaAs semiconductor layer on one of the inner walls of the cavity, a multi GHz mode locked laser and a lens system to ensure uniform illumination of the surface. The dimensions of the super-conducting Nb microwave cavity is chosen such that it has $\mathbf{TE_{101}}$ mode frequency of 2.5 GHz. The transverse dimensions are y = 71 mm and z = 22 mm and the length of the cavity is x = 110 mm. The Q-factor of the cavity is 10^6. The cavity is constantly immersed in Liquid He Bath. A GaAs semiconductor layer with a thickness of δx = 0.3 mm is coated on the inner yz-wall of the super-conducting cavity. This wall is uniformly illuminated by the laser beam. The wavelength of the laser beam is chosen such that it is equal to the band gap of the semiconductor.

The laser source emits pulses at 5 GHz frequency with a pulse duration less that 10 ps and an average power of 12-20 mW. A single run produces a train of $10^4 - 10^5$ pulses. The presence of the semiconductor layer in the cavity does not affect the Q-factor of the cavity.

In the absence of the laser pulse on the semiconductor surface, modes are formed with vanishing boundary conditions on the surface of the super-conductor. Hence, on the surface of the semi-conductor, there will be non-vanishing tangential electric and magnetic fields corresponding to the $\mathbf{TE_{101}}$ mode given by $\mathbf{E_t}$ and $\mathbf{H_t}$ respectively. This leads to a non vanishing surface impedence ζ given by

$$\mathbf{E_t} = \zeta(\mathbf{H_t} \times \hat{\mathbf{n}}) \tag{3.24}$$

Whenever a cavity has a non-vanishing surface impedence, there is a frequency shift in the cavity given by

$$\Delta\tilde{\omega} = \Delta\omega - \frac{i\Gamma}{2} = -\frac{ic}{2}\frac{\int\int \zeta|\mathbf{H_t}|^2 \mathbf{d\Sigma}}{\int\int\int |\mathbf{H_t}|^2 \mathbf{d\Omega}} \tag{3.25}$$

When the semiconductor slab is illuminated by the laser pulse, it excites the electrons in the valence band into the conduction band and the semiconductor perfectly reflects microwave, resulting in zero surface impedence ($\zeta = 0$). This implies that the frequency of the cavity changes from $\omega_0 + \Delta\tilde{\omega}$ to ω_0 and vice versa with a frequency of the laser pulse. A schematic view of the process involved is shown in Fig.(3.2). The frequency of the laser pulse is chosen such that it is twice the cavity frequency. This condition ensures parametric resonance of the $\mathbf{TE_{101}}$ modes in the cavity as required to observe dynamic casimir effect. The photons generated from the vacuum by this process are detected by the detector. The sensitivity of the detector is sufficient to detect 1000 microwave photons.

3.2 General Theory

3.2.1 Lagrangian Circuit Description

Our purpose in this section is to provide a Lagrangian description of a single microwave cavity mode[36] which follows from the action principle formulation of electrodynamics. For this purpose we employ the Coulomb gauge, for the vector potential: $div\mathbf{A}_{mode} = 0$. The vector potential representing the cavity mode may be written

$$\mathbf{A}_{mode}(\mathbf{r}, t) = \Phi(t)\mathbf{K}(\mathbf{r}). \tag{3.26}$$

The mode electromagnetic fields are then given by

$$\begin{aligned} \mathbf{E}_{mode}(\mathbf{r}, t) &= -\frac{1}{c}\left[\frac{\partial \mathbf{A}_{mode}(\mathbf{r}, t)}{\partial t}\right] = -\frac{\dot{\Phi}(t)}{c}\mathbf{K}(\mathbf{r}), \\ \mathbf{B}_{mode}(\mathbf{r}, t) &= curl\mathbf{A}_{mode}(\mathbf{r}, t) = \Phi(t)\ curl\mathbf{K}(\mathbf{r}). \end{aligned} \tag{3.27}$$

The Lagrangian

$$L_{field} = \frac{1}{8\pi}\int_{cavity}\left[|\mathbf{E}_{mode}(\mathbf{r}, t)|^2 - |\mathbf{B}_{mode}(\mathbf{r}, t)|^2\right] d^3\mathbf{r} \tag{3.28}$$

describes the mode in terms of a simple oscillator circuit. The capacitance C and inductance Λ of the circuit are defined, respectively, by

$$\begin{aligned} C &= \frac{1}{4\pi}\int_{cavity}|\mathbf{K}(\mathbf{r})|^2\, d^3\mathbf{r}, \\ \frac{1}{\Lambda} &= \frac{1}{4\pi}\int_{cavity}|curl\mathbf{K}(\mathbf{r})|^2\, d^3\mathbf{r}. \end{aligned} \tag{3.29}$$

The circuit electromagnetic field Lagrangian follows from Eqs.(3.27), (3.28) and (3.29). It is of the simple ΛC oscillator form

$$L_{field}(\dot{\Phi}, \Phi) = \frac{C}{2c^2}\dot{\Phi}^2 - \frac{1}{2\Lambda}\Phi^2, \tag{3.30}$$

wherein the bare circuit frequency obeys

$$\Omega_\infty^2 = \frac{c^2}{\Lambda C} \ . \tag{3.31}$$

The interactions between cavity wall currents and an electromagnetic mode are conventionally described by

$$\begin{aligned} L_{int} &= \frac{1}{c}\int \mathbf{J}\cdot\mathbf{A}_{mode} d^3\mathbf{r}, \\ L_{int} &= \frac{1}{c} I\Phi, \\ I(t) &= \int \mathbf{J}(\mathbf{r},t)\cdot\mathbf{K}(\mathbf{r}) d^3\mathbf{r}, \end{aligned} \tag{3.32}$$

where the current I drives the oscillator circuit.

In total, the circuit mode Lagrangian follows from Eqs.(3.30) and (3.32) as

$$L = \frac{C}{2c^2}\dot{\Phi}^2 - \frac{1}{2\Lambda}\Phi^2 + \frac{1}{c}I\Phi + L' \tag{3.33}$$

wherein L' describes all of the other degrees of freedom which couple into the mode coordinate. Maxwell's equations for a single microwave mode then take the form

$$\begin{aligned} \frac{d}{dt}\left(\frac{\partial L}{\partial \dot{\Phi}}\right) &= \left(\frac{\partial L}{\partial \Phi}\right), \\ C\left(\ddot{\Phi} + \Omega_\infty^2 \Phi\right) &= cI. \end{aligned} \tag{3.34}$$

The damping of the oscillator will first be discussed from a classical electrical engi-

neering viewpoint and only later from a fully quantum electrodynamic viewpoint.

3.2.2 Oscillator Circuit Damping

From an electrical engineering viewpoint[37], let us consider a small external current source δI_{ext} which drives the mode coordinate $\delta\Phi$. Eq.(3.34) now reads

$$\frac{C}{c^2}\delta\ddot{\Phi} + \frac{1}{\Lambda}\delta\Phi = \frac{1}{c}\delta I = \frac{1}{c}\left(\delta I_{ext} + \delta I_{ind}\right) \tag{3.35}$$

were δI_{ind} is the current induced by the coordinate response $\delta\Phi$. In the complex frequency ζ domain we have in (the upper half $\Im m\ \zeta > 0$ plane)

$$\begin{aligned} \delta I_{ext}(t) &= \Re e\left\{\delta I_{ext,\zeta} e^{-i\zeta t}\right\} \\ \delta\Phi(t) &= \Re e\left\{\delta I_{ext,\zeta}\mathcal{D}(\zeta) e^{-i\zeta t}\right\}. \end{aligned} \tag{3.36}$$

The induced current is determined by the "surface admittance" $Y(\zeta)$ of the cavity walls; In detail

$$\begin{aligned} \delta I_{ind}(t) &= -\frac{1}{c}\int_0^\infty \mathcal{G}(t')\delta\dot{\Phi}(t-t')dt', \\ Y(\zeta) &= \int_0^\infty e^{i\zeta t}\mathcal{G}(t)dt, \end{aligned} \tag{3.37}$$

so that

$$\begin{aligned} \left\{-\frac{C}{c^2}\zeta^2 + \frac{1}{\Lambda} - \frac{i\zeta}{c^2}Y(\zeta)\right\}\mathcal{D}(\zeta) &= \frac{1}{c}\ , \\ -i\zeta\varepsilon(\zeta)C &= -i\zeta C + Y(\zeta), \end{aligned} \tag{3.38}$$

wherein the effective frequency dependent capacitance $\varepsilon(\zeta)C$ determines the mode dielectric response function $\varepsilon(\zeta)$. The retarded propagator for the mode in the

frequency domain obeys[25, 36]

$$\mathcal{D}(\zeta) = \frac{\Lambda}{c}\left[\frac{\Omega_\infty^2}{\Omega_\infty^2 - \zeta^2 - \Pi(\zeta)}\right] \tag{3.39}$$

wherein the "self energy" $\Pi(\zeta)$, or equivalently the "damping function" $\Gamma(\zeta)$, is determined by the induced current admittance via

$$\Pi(\zeta) = \frac{i\zeta Y(\zeta)}{C} = \Pi(0) + i\zeta\Gamma(\zeta). \tag{3.40}$$

The self energy describes both frequency shift and damping properties of the mode.

Causality dictates that all engineering response functions obey analytic dispersion relations ($\Im m\ \zeta > 0$) of the form

$$\begin{aligned} \mathcal{D}(\zeta) &= \frac{2}{\pi}\int_0^\infty \frac{\omega \Im m \mathcal{D}(\omega + i0^+) d\omega}{\omega^2 - \zeta^2}\ , \\ \Pi(\zeta) &= \frac{2}{\pi}\int_0^\infty \frac{\omega \Im m \Pi(\omega + i0^+) d\omega}{\omega^2 - \zeta^2}\ . \end{aligned} \tag{3.41}$$

The damping rate for the oscillation is determined by

$$\Im m \Pi(\omega + i0^+) = \omega \Re e \Gamma(\omega + i0^+) = \frac{\omega \Re e Y(\omega + i0^+)}{C}\ . \tag{3.42}$$

The shifted frequency,

$$\Omega_0^2 = \Omega_\infty^2 - \Pi(0), \tag{3.43}$$

is related to the damping rate via the dispersion relation sum rule[25]

$$\Omega_\infty^2 = \Omega_0^2 + \frac{2}{\pi}\int_0^\infty \Re e \Gamma(\omega + i0^+) d\omega, \tag{3.44}$$

which follows from Eqs.(3.40) - (3.43). Finally, the quality factor Q for the mode

frequency Ω_0 is well defined as

$$\frac{\Omega_0}{Q} = \Re e\Gamma(\Omega_0 + i0^+) \tag{3.45}$$

if and only if the mode is under damped by a large margin; e.g. $Q \gg 1$. From Eq.(3.43), we see that if the damping is sufficiently strong ($\Pi(0) > \Omega_\infty^2$), then the mode can go unstable as alluded to in the introduction. Let us consider this physical effect in more detail.

3.2.3 Dynamical Casimir Effects

We now turn to a discussion of the dynamical Casimir effect[37] and introduce the notion of a *noise* temperature. In the linear regime considered in this section, the dynamical Casimir effect is shown to be directly related to the production of a pair of photons.

Suppose that the dielectric response function $\varepsilon(\zeta)$ of the mode in Eq.(3.38) is made to vary with time; i.e.

$$\varepsilon(\zeta) \;\Rightarrow\; \varepsilon(\zeta, t) \;\text{ equivalently }\; \Pi(\zeta) \;\Rightarrow\; \Pi(\zeta, t). \tag{3.46}$$

If the resulting differential equation for the $\Phi = \Re e\{\phi\}$ signal is linear (to a sufficient degree of accuracy)

$$\begin{aligned} \ddot{\phi}(t) + \Omega^2(t)\phi(t) &= 0, \\ \Omega(t \to \pm\infty) &= \Omega_0, \end{aligned} \tag{3.47}$$

then there exists a solution of the form

$$\phi(t \to \infty) = e^{i\Omega_0 t} + \rho e^{-i\Omega_0 t},$$
$$\phi(t \to -\infty) = \sigma e^{i\Omega_0 t},$$
$$|\rho|^2 + |\sigma|^2 = 1. \tag{3.48}$$

From a quantum mechanical viewpoint, the time variation $e^{i\Omega_0 t}$ may represent a photon moving backward in time and $e^{-i\Omega_0 t}$ may represent photon moving forward in time. In Eq.(3.48), the reflection amplitude for a photon moving backward in time to bounce forward in time is given by ρ. A backward in time moving photon reflected forward in time appears in the laboratory to be a pair of photons being created[31, 38].

The probability of such a photon pair creation event defines a *photon pair creation noise temperature* T^* induced by the time varying frequency via

$$R = |\rho|^2 = e^{-\hbar\Omega_0/k_B T^*}. \tag{3.49}$$

The mean number $\bar{N}$ of photons which would be radiated from the vacuum by a time varying frequency modulation $\Omega(t)$ obeys a formal Planck law

$$\bar{N} = \frac{R}{1-R} = \frac{1}{e^{\hbar\Omega_0/k_B T^*} - 1} \ . \tag{3.50}$$

Suppose (for example) that a microwave cavity is initially in thermal equilibrium at temperature T_i. The mean number of initial microwave photons in a given normal mode is then given by

$$N_i = \frac{1}{e^{\hbar\Omega_0/k_B T_i} - 1} \ . \tag{3.51}$$

After a sequence of frequency modulation pulses the mean number of final photons

in the cavity mode is

$$N_f = (2\bar{N}+1)N_i + \bar{N} = N_i \coth\left(\frac{\hbar\Omega_0}{2k_B T^*}\right) + \frac{1}{e^{\hbar\Omega_0/k_B T^*} - 1} \ . \tag{3.52}$$

Note that the existence of an *initial* number of photons N_i in the cavity mode makes larger the final number of photons

$$N_f = \frac{1}{e^{\hbar\Omega_0/k_B T_f} - 1} \tag{3.53}$$

via the *induced* radiation of additional photon pairs. If the microwave frequency large margin inequality

$$\hbar\Omega_0 \ll k_B T^* \tag{3.54}$$

holds true, then Eqs.(3.50) - (3.54) imply the following approximate law for the *final* cavity mode noise temperature

$$T_f \approx T^* \coth\left(\frac{\hbar\Omega_0}{2k_B T_i}\right). \tag{3.55}$$

The dynamical Casimir effect for frequency modulation pulses is thereby described in terms of the amount of heat that raises the temperature $T_i \to T_f$ of the microwave cavity. In the next section, we consider periodic frequency modulations in detail.

3.2.4 Periodic Frequency Modulation

For periodic modulations in the frequency[37], one must examine[39] the differential equation

$$\begin{aligned}\ddot{\phi}(t) + \Omega^2(t)\phi(t) &= 0,\\ \Omega^2(t) &= \Omega_0^2 + \nu^2(t),\\ \nu(t+\tau) &= \nu(t).\end{aligned} \tag{3.56}$$

From a mathematical viewpoint, Eq.(3.56) has been well studied. If $\nu(t)$ can be represented as a non-overlapping pulse sequence of the form

$$\nu(t) = \sum_{n=-\infty}^{\infty} \varpi(t - n\tau), \tag{3.57}$$

then the transmission problem for a single pulse,

$$\ddot{\phi}_1(t) + \{\Omega_0^2 + \varpi^2(t)\}\phi_1(t) = 0, \tag{3.58}$$

yields a complete solution to the general problem. In particular, we examine the two photon creation problem as in Eq.(3.48); i.e.

$$\begin{aligned}\phi_1(t \to \infty) &= e^{i\Omega_0 t} + \rho_1 e^{-i\Omega_0 t},\\ \phi_1(t \to -\infty) &= \sigma_1 e^{i\Omega_0 t},\\ |\rho_1|^2 + |\sigma_1|^2 &= R_1 + P_1 = 1,\\ \sigma_1 &= \sqrt{P_1}\; e^{-i\Theta_1}.\end{aligned} \tag{3.59}$$

Employing the characteristic function

$$\mu(\Omega_0) = \frac{\cos(\Omega_0\tau + \Theta_1(\Omega_0))}{\sqrt{P_1(\Omega_0)}}, \tag{3.60}$$

one may study the stability problem for the dynamic Casimir effect. For *periodic* frequency modulations there are two cases of interest[31]:

Case I: *Stable Motions* $-1 < \mu(\Omega_0) < +1$

$$\begin{aligned} \mu(\Omega_0) &= \cos(\Omega\tau) \\ \phi_\pm(t+\tau) &= e^{\pm i\Omega t}\phi_\pm(t). \end{aligned} \tag{3.61}$$

Case II: *Unstable Motions* $\mu(\Omega_0) > +1$ or $\mu(\Omega_0) < -1$

$$\begin{aligned} \mu(\Omega_0) = \cosh(\gamma\tau) \quad \text{or} \quad \mu(\Omega_0) &= -\cosh(\gamma\tau) \\ \phi_\pm(t+\tau) &= e^{\pm\gamma t}\phi_\pm(t). \end{aligned} \tag{3.62}$$

In the unstable regime, 2γ represents the number of cavity photons being produced per unit time. If the cavity mode has a high quality factor $Q \gg 1$, then photons are also absorbed at a rate (Ω_0/Q). The net photon production rate in this approximation would then be

$$\Gamma_1 \simeq \left(2\gamma - \frac{\Omega_0}{Q}\right), \tag{3.63}$$

and the theoretical noise temperature after n_p pulses would be

$$k_B T_1^* \approx \hbar\Omega_0 \exp(n_p\tau\Gamma_1). \tag{3.64}$$

As an example, let us suppose a sequence of rectangular pulse sequences of the form

$$\Omega(t) = \Omega_0 \quad \text{if} \quad t_0 + n\tau < t < t_0 + (n + 1/2)\tau,$$
$$\Omega(t) = (1 + \alpha)\Omega_0 \quad \text{if} \quad t_0 + (n + 1/2)\tau < t < t_0 + (n + 1)\tau, \tag{3.65}$$

wherein $n = 1, 2, \ldots, n_p$. The estimate

$$\exp(n_p \tau \Gamma_1) \sim \exp(n_p \alpha/2) \quad \text{for} \quad 1 \gg \alpha \gg (\Omega_0 \tau)/Q \tag{3.66}$$

is not unreasonable.

Eq.(3.66) shows the inherent instability present in the dynamical Casimir effect since for case II, the number of produced photons increases exponentially. In fact, were it not controlled, the exponential temperature *instability* for high quality cavity modes, i.e. $\Gamma_1 > 0$ in Eqs.(3.63) - (3.66), would be sufficient for large n_p to *melt* the cavity. No microwave oven works that efficiently even if the dynamic Casimir effect were employed for exactly that purpose. The one loop photon approximation is evidently at fault and higher loops (non-linear processes) must be invoked for the noise temperature of the mode to be theoretically stable as would be laboratory microwave cavities.

Once again an analogy might be helpful (this time with lasers). The master equation for an *ideal* laser with a production rate γ_o satisfies the linear differential equation

$$\frac{dn(t)}{dt} = \gamma_o n(t), \tag{3.67}$$

whose solution leads to an exponentially large number of photons n for large t. This un-physical growth is curtailed through considerations of non-linear processes which leads to *saturation* in the mean number of produced photons. The more

correct equation reads

$$\frac{d\hat{n}(t)}{dt} = \gamma_o \hat{n}(t) - \gamma_1 \hat{n}^2(t), \tag{3.68}$$

and leads to saturation with a mean number $\bar{n} = \frac{\gamma_o}{\gamma_1}$. Theoretically, one would calculate γ_o and γ_1 in different orders of loop perturbation theory. In the next section, we shall develop a similar strategy to obtain saturation and an explicit, finite expression for the mean number of produced photons.

3.3 Application to the Proposed Cavity Experiment

3.3.1 Photon Generation Rates

The cavity frequency[31] of a rectangular cavity $(x(t), y, z)$, where one of the dimensions of the cavity is time dependent, is given by

$$\omega_k(t) = \pi c \left[\left(\frac{l}{x(t)} \right)^2 + \left(\frac{m}{y} \right)^2 + \left(\frac{n}{z} \right)^2 \right]^{\frac{1}{2}} \tag{3.69}$$

The Hamiltonian for a single mode in terms of the photon oscillator coordinates are given by

$$H(t) = \frac{1}{2} \left[P^2 + \omega_k(t)^2 Q^2 \right] \tag{3.70}$$

The creation and the annihilation operators are given by

$$\begin{aligned} a^\dagger(t) &= \left[\frac{\omega_k(t)}{2\hbar} \right]^{\frac{1}{2}} Q(t) - i \left[\frac{1}{2\omega_k(t)\hbar} \right]^{\frac{1}{2}} P(t) \\ a(t) &= \left[\frac{\omega_k(t)}{2\hbar} \right]^{\frac{1}{2}} Q(t) + i \left[\frac{1}{2\omega_k(t)\hbar} \right]^{\frac{1}{2}} P(t) \end{aligned} \tag{3.71}$$

and $\left[a(t), a^{\dagger}(t)\right] = 1$. Equation 3.69 now becomes

$$H(t) = \frac{1}{2}\left[a(t)a^{\dagger}(t) + \frac{1}{2}\right] \tag{3.72}$$

If the system evolves from an initial time t_1, the number of photons at time t_2 is given by

$$N(t_2) = \langle 0, t_1 | a^{\dagger}(t_2) a(t_2) | 0, t_1 \rangle \tag{3.73}$$

If one introduces a variable $q_k(t)$, where

$$Q_k(t) = q_k(t) + q_k^*(t) \tag{3.74}$$

then it can be shown that $q_k(t)$ obey the equation

$$\frac{d^2}{dt^2} q_k(t) + \omega_k^2(t) q_k(t) = 0 \tag{3.75}$$

where $\omega(t)$ is assumed to be time dependent over a finite time interval $-T < t < +T$ and $\omega(t) = \omega_i$ for $t < -T$ and $\omega(t) = \omega_f$ for $t > +T$. For the sake of simplicity, we can assume that $\omega_i = \omega_f$. The differential equation3.75 has two solutions given by

$$\begin{aligned} q_f(t) &= \exp -i\omega t + R_b(\omega) \exp(+i\omega t) \\ &= T_f(\omega) \exp(-i\omega t) \end{aligned} \tag{3.76}$$

and

$$\begin{aligned} q_b(t) &= T_b(\omega) \exp(+i\omega t) \\ &= \exp +i\omega t + R_f(\omega) \exp(-i\omega t) \end{aligned} \tag{3.77}$$

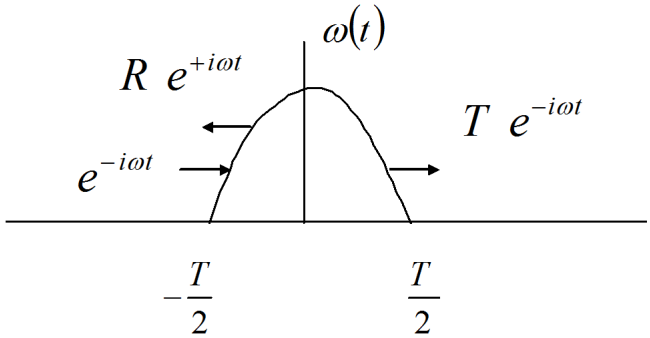

The average number of photons produced is $N = \dfrac{|R\ (\omega)|^2}{1-|R\ (\omega)|^2}$

Figure 3.3: Reflection of photon in time

These two equations are not linearly independent, as the Wronskian given by

$$W[q_1, q_2] = q_1 \frac{dq_2}{dt} - \frac{dq_1}{dt} q_2 = constant \tag{3.78}$$

Upon evaluating the Wronskian $W[Q, q_b]$ for $t_1 < -T$ and for $t_2 > +T$ (Q is given by Eq.(3.74))and equating the results, one gets the expression for $a(t_2)$ as

$$a(t_2) = \frac{T_b \exp(i\omega t_1) a(t_1) + T_b^* R_f \exp(-i\omega t_1) a^\dagger(t_1)}{\exp i\omega t_2\,(1 - |R_f|^2)} \tag{3.79}$$

Using this equation in Eq.(3.73) one gets the final expression for the number of

photons as

$$N_k(\omega) = \frac{|R_{fk}(\omega)|^2}{1 - |R_{fk}(\omega)|^2} = \frac{|R_{bk}(\omega)|^2}{1 - |R_{bk}(\omega)|^2} \tag{3.80}$$

where R_{fk}, R_{bk} depends on the shape of $\omega^2(t)$ as a function of time (Fig.(3.3)).

In deriving the above expression, we had assumed that $\omega(t)$ was varying over an interval $-T < t < +T$. If instead, $\omega(t)$ was periodic function of time such that $\omega(t) = \omega_2$ for $-T_2 < t < +T_2$,$\omega(t) = \omega_1$ for $T_2 < t < T_2 + 2T_1$ and periodic with a period $T = 2T_1 + 2T_2$, one needs to solve Eq.(3.75) for this particular $\omega(t)$.After modulating the frequency for a time $t = r\Delta T$, where r is a large integer, in the region where $\omega(t) = \omega_1$, the modes are given by

$$q_r(t) = A_r \exp i\omega_1(t - rT) + B_r \exp -i\omega_1(t - rT) \tag{3.81}$$

The coefficients A_r, B_r are related to A_{r+1}, B_{r+1} via a transfer matrix P given by

$$P = \begin{pmatrix} (\alpha_1 - i\beta_1)e^{i\omega T} & -i\beta_2 e^{i\omega T} \\ i\beta_2 e^{-i\omega T} & (\alpha_1 + i\beta_1)e^{-i\omega T} \end{pmatrix} \tag{3.82}$$

where

$$\begin{aligned} \alpha_1 &= \cos(2\omega_2 T_2)\cos(2\omega T_2) + \frac{\epsilon}{2}\cos(2\omega_2 T_2)\cos(2\omega T_2) \\ \beta_1 &= \sin(2\omega T_2)\cos(2\omega_2 T_2) - \frac{\epsilon}{2}\sin(2\omega_2 T_2)\cos(2\omega T_2) \\ \beta_2 &= \frac{\eta}{2}\sin(2\omega_2 T_2) \end{aligned} \tag{3.83}$$

and

$$\begin{aligned} \epsilon &= \frac{\omega_2}{\omega} + \frac{\omega}{\omega_2} \\ \eta &= \frac{\omega_2}{\omega} - \frac{\omega}{\omega_2} \end{aligned} \tag{3.84}$$

Here $\alpha_1, \beta_1, \beta_2$ satisfy the condition

$$\alpha_1^2 + \beta_1^2 - \beta_2^2 = 1 \tag{3.85}$$

If one starts with a mode q_0 defined by A_0, B_0 then the coefficients A_r, B_r which defines the mode q_r are given by

$$\begin{pmatrix} A_r \\ B_r \end{pmatrix} = P^r \begin{pmatrix} A_0 \\ B_0 \end{pmatrix} = U P_d^r U^{-1} \begin{pmatrix} A_0 \\ B_0 \end{pmatrix} \tag{3.86}$$

where,P_d is a diagonal matrix constituting the eigenvalues of P. The eigenvalues of P are determined by the characteristic equation

$$\begin{aligned} p^2 - pTr(P) + \det(P) = 0 \\ p_\pm = \frac{1}{2}\left[Tr(P) \pm \sqrt{[Tr(P)]^2 - 4}\right] \end{aligned} \tag{3.87}$$

Acceptable solutions are obtained only if $p_\pm$ are complex conjugates. Defining a real parameter γ, such that

$$\cos(\gamma) = \frac{1}{2}Tr(P) = \alpha_1 \cos(\omega T) + \beta \sin(\omega T) \text{ with } \quad p_\pm = e^{\pm i\gamma} \tag{3.88}$$

The U matrix takes the form

$$U = \begin{pmatrix} p_+ e^{i\omega T} - A & p_- e^{i\omega T} - A \\ i\beta_2 & i\beta_2 \end{pmatrix} \tag{3.89}$$

Using Eqs.(3.76), (3.77) and (3.86), we have

$$\begin{pmatrix} 1 \\ R_f \end{pmatrix} = U P_d^r U^{-1} \begin{pmatrix} T_b \\ 0 \end{pmatrix} \tag{3.90}$$

Using this equation we can obtain an expression for $|R_f|^2$ is given by

$$|R_f|^2 = \frac{\beta_2^2}{\alpha_1^2 + \beta_1^2 - 2B\cos(\gamma) + B^2} \quad \text{where} \quad B = \frac{\sin((r+1)\gamma)}{\sin(r\gamma)} \tag{3.91}$$

If one assumes that $T_1 = T_2 = \frac{T}{4}$, we have

$$\cos(\gamma) = \cos\left(\frac{\omega_2 T}{2}\right)\cos\left(\frac{\omega T}{2}\right) - \frac{1}{2}\left(\frac{\omega_2}{\omega} + \frac{\omega}{\omega_2}\right)\sin\left(\frac{\omega_2 T}{2}\right)\sin\left(\frac{\omega T}{2}\right)$$

Using Eqs.(3.80),(3.83),(3.84),(3.85),(3.91) and (3.92) we have the final expression for the number of photons as

$$N = \frac{1}{4}\left[\frac{\omega}{\omega_2} - \frac{\omega_2}{\omega}\right]^2 \sin^2\left(\frac{\omega_2 T}{2}\right)\frac{\sin^2(r\gamma)}{\sin^2(\gamma)} \tag{3.92}$$

3.3.2 Calculation of Frequency Shifts in the Cavity

The transition rate per unit time for photon absorption[40] is given by

$$\Gamma = \frac{c^2}{4\pi}\left(\frac{\iint_\Sigma Re\left(Z(\omega)\right) \mid H_\omega \mid^2 \, \mathrm{d}\Sigma}{\iiint_\Omega \mid H_\omega \mid^2 \, \mathrm{d}\Omega}\right) \tag{3.93}$$

Where Σ is the boundary of the cavity where disspipation (or absorption) of photons occur and Ω is the volume of the entire cavity under consideration and Z is the surface impedence of the cavity which is, in general, complex number.

The Frequency shift is given by,

$$\Delta\tilde{\omega} = \Delta\omega - \frac{i\Gamma}{2} = -\frac{ic^2}{8\pi}\left(\frac{\iint_\Sigma Z(\omega + i0^+) \mid H_\omega \mid^2 \, \mathrm{d}\Sigma}{\iiint_\Omega \mid H_\omega \mid^2 \, \mathrm{d}\Omega}\right) \tag{3.94}$$

Since, $R_{vac} = \frac{4\pi}{c}$, we have,

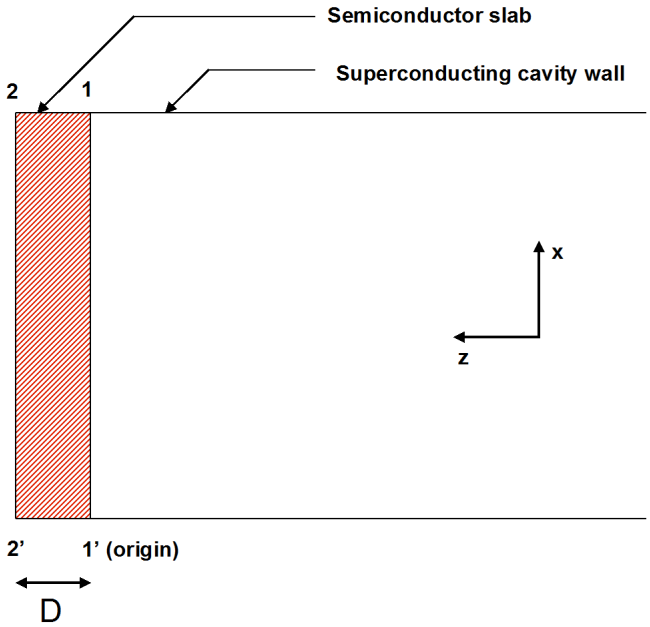

Figure 3.4: Geometry for calculating surface impedence

$$\Delta\tilde{\omega} = \Delta\omega - \frac{i\Gamma}{2} = -\frac{ic}{2}\left(\frac{\iint_{\Sigma}\left(\frac{Z(\omega+i0^{+})}{R_{vac}}\right) \mid H_{\omega} \mid^{2} \ \mathrm{d}\Sigma}{\iiint_{\Omega} \mid H_{\omega} \mid^{2} \ \mathrm{d}\Omega}\right) \tag{3.95}$$

The surface impedance is defined as $\zeta = \frac{Z}{R_{vac}}$ and satisfies the following relation on the boundary surface.

$$\mathbf{E_t} = \zeta \mathbf{H_t} \times \mathbf{n} \tag{3.96}$$

where $\mathbf{E_t}$ and $\mathbf{H_t}$ are the tangential Electric and Magnetic fields, respectively, at the boundary. For the case under consideration (Fig.(3.4)), plane wave in medium A is incident on the medium B (the interface being 1-1'), travels a distance 'D' gets reflected (totally)(the interface being 2-2'). The surface impedance at the

boundary 1-1' needs to be calculated (The incident E-Field is along the x-direction, the propagation is along the z-direction and the origin is in the 1-1' interface). Wave equations as functions of z(the wave is propagating in the z-direction):

$$\begin{aligned}\mathbf{E}_{I1}(z) = E_{I1}e^{-ik_1z}\hat{\mathbf{e_x}}; \quad \mathbf{E}_{R1}(z) = E_{R1}e^{+ik_1z}\hat{\mathbf{e_x}} \\ \mathbf{E}_{I2}(z) = E_{I2}e^{-ik_2z}\hat{\mathbf{e_x}}; \quad \mathbf{E}'_{I2}(z) = E'_{I2}e^{+ik_2z}\hat{\mathbf{e_x}}\end{aligned} \tag{3.97}$$

Maxwell's Equations in charge free space are given by

$$\omega\mu\mathbf{H} = c\mathbf{k}\times\mathbf{E}; \omega\epsilon\mathbf{E} = -c\mathbf{k}\times\mathbf{H} \tag{3.98}$$

Taking $\mu = 1$,

$$\omega\mathbf{H} = c\mathbf{k}\times\mathbf{E} \tag{3.99}$$

In terms of the components of the field under consideration,

$$\begin{aligned}\mathbf{H}_{I1}(z) = \frac{c}{\omega}k_1E_{I1}(z)\hat{\mathbf{e_y}}; \quad \mathbf{H}_{R1}(z) = -\frac{c}{\omega}k_1E_{R1}(z)\hat{\mathbf{e_y}} \\ \mathbf{H}_{I2}(z) = \frac{c}{\omega}k_2E_{I2}(z)\hat{\mathbf{e_y}}; \quad \mathbf{H}'_{I2}(z) = -\frac{c}{\omega}k_1E'_{I2}(z)\hat{\mathbf{e_y}}\end{aligned} \tag{3.100}$$

Boundary conditions for the electric field at the interface $1-1'(z=0)$ and at the interface $2-2'(z=D)$ are ,

$$\begin{aligned}E_{I1}(0) + E_{R1}(0) &= E_{I2}(0) + E'_{I2}(0) \quad \text{and} \\ E_{I2}(D) + E'_{I2}(D) &= 0\end{aligned} \tag{3.101}$$

respectively. Together, they yield the relation,

$$E_{I1} + E_{R1} = E_{I2}\left(1 - e^{-2ik_2D}\right) \tag{3.102}$$

Boundary Condition for the H-fields at the interface $1-1'(z=0)$

$$H_{I1}(0)+H_{R1}(0)=H_{I2}(0)+H'_{I2}(0) \tag{3.103}$$

together with the relations derived for E-fields yield,

$$E_{I1}-E_{R1}=\frac{k_2}{k_1}E_{I2}\left(1+e^{-2ik_2D}\right) \tag{3.104}$$

The Tangential E-Fields at the $1-1'$ interface:

$$\begin{aligned}\mathbf{E}_t &= (\mathbf{E}_{I1}+\mathbf{E}_{R1}) \\ &= E_{I2}\left(1-e^{-2ik_2D}\right)\hat{\mathbf{x}}\end{aligned} \tag{3.105}$$

The Tangential H-Fields at the $1-1'$ interface:

$$\begin{aligned}\mathbf{H}_t &= \mathbf{H}_{I1}+\mathbf{H}_{R1} \\ &= \frac{c}{\omega}k_2E_{I2}\left(1+e^{-2ik_2D}\right)\hat{\mathbf{y}}\end{aligned} \tag{3.106}$$

Using Eqs.(3.96), (3.105) and (3.106), we have

$$\zeta=\frac{\omega}{c}\frac{1}{k_2}i\tan\left(k_2D\right) \tag{3.107}$$

If we put $k_2 = u + iv$, we get

$$\begin{aligned}
\Re(\zeta) &= \frac{\omega D}{c}\frac{1}{u^2+v^2}\frac{(v\sin(2u) - u\sinh(2v))}{\cos(2u)+\cosh(2v)} \\
\Im(\zeta) &= \frac{\omega D}{c}\frac{1}{u^2+v^2}\frac{(u\sin(2u) + v\sinh(2v))}{\cos(2u)+\cosh(2v)} \qquad \text{where} \\
u &= \frac{\omega D}{c}\sqrt{\left(\frac{\epsilon}{2}\right)}\left(\left(1+\left(\frac{4\pi\sigma}{\epsilon\omega}\right)^2\right)^{\frac{1}{2}}+1\right)^{\frac{1}{2}} \\
v &= \frac{\omega D}{c}\sqrt{\left(\frac{\epsilon}{2}\right)}\left(\left(1+\left(\frac{4\pi\sigma}{\epsilon\omega}\right)^2\right)^{\frac{1}{2}}-1\right)^{\frac{1}{2}}
\end{aligned} \tag{3.108}$$

From Eq.(3.97) the frequency shift is given by,

$$\Delta\omega = \frac{c}{2}\Im(\zeta)\left(\frac{\iint_\Sigma \mid H_\omega \mid^2 \ \mathrm{d}\Sigma}{\iiint_\Omega \mid H_\omega \mid^2 \ \mathrm{d}\Omega}\right) \tag{3.109}$$

For a cuboidal resonant cavity with a = 110mm, b = 71mm, h = 22mm, with TE_{101} mode, the fields inside the cavity are,

$$\begin{aligned}
E_x &= E_z = 0 \\
E_y &= A_1 \sin\left(\frac{\pi x}{a}\right)\sin\left(\frac{\pi z}{h}\right)
\end{aligned} \tag{3.110}$$

and

$$\begin{aligned}
H_x &= -\frac{ic}{\omega}A_1\frac{\pi}{h}\sin\left(\frac{\pi x}{a}\right)\cos\left(\frac{\pi z}{h}\right) \\
H_y &= 0; \\
H_z &= -\frac{ic}{\omega}A_1\frac{\pi}{a}\cos\left(\frac{\pi x}{a}\right)\sin\left(\frac{\pi z}{h}\right)
\end{aligned} \tag{3.111}$$

The volume integral can be evaluated to be,

$$\int_V \mid H \mid^2 \mathrm{d}V = -\frac{c^2\pi^2}{\omega^2} A_1^2 \left[\frac{1}{h^2}\frac{abh}{4} + \frac{1}{a^2}\frac{abh}{4} \right] \tag{3.112}$$

Semiconductor is coated in the $y-z$ plane at $x=0$. So, the surface integral has to be evaluated only on this surface.

$$\begin{aligned} \iint_S \mid H_{tan} \mid^2 \mathrm{d}S &= \int_0^h \int_0^b \mid H_z \mid^2 \mathrm{d}y\mathrm{d}z \\ &= -\frac{A_1^2\pi^2c^2}{\omega^2}\frac{1}{a^3}\left[\frac{abh}{2}\right] \end{aligned} \tag{3.113}$$

The frequency shift can now be written in the final form as

$$\begin{aligned} \Delta\omega &= \frac{c}{2}\frac{\omega D}{c}\frac{1}{u^2+v^2}\frac{[u\sin(2u)+v\sinh(2v)]}{\cos(2u)+\cosh(2v)}\left(\frac{\frac{2}{a^3}}{\frac{1}{a^2}+\frac{1}{h^2}}\right) \quad \text{where} \\ u &= \frac{\omega D}{c}\sqrt{\left(\frac{\epsilon}{2}\right)}\left(\left(1+\left(\frac{4\pi\sigma}{\epsilon\omega}\right)^2\right)^{\frac{1}{2}}+1\right)^{\frac{1}{2}} \\ v &= \frac{\omega D}{c}\sqrt{\left(\frac{\epsilon}{2}\right)}\left(\left(1+\left(\frac{4\pi\sigma}{\epsilon\omega}\right)^2\right)^{\frac{1}{2}}-1\right)^{\frac{1}{2}} \end{aligned} \tag{3.114}$$

The special cases for the frequency shifts corresponding to zero and infinite conductivity are,

$$\begin{aligned} \Delta\omega &= \frac{c}{\sqrt{\epsilon}}\tan\left(\frac{\omega D}{c}\sqrt{\epsilon}\right)\left(\frac{\frac{1}{a^3}}{\frac{1}{a^2}+\frac{1}{h^2}}\right) \quad \text{and} \\ \Delta\omega' &= \frac{c}{2}\sqrt{\frac{\omega}{2\pi\sigma}}\left(\frac{\frac{1}{a^3}}{\frac{1}{a^2}+\frac{1}{h^2}}\right) \approx 0 \end{aligned} \tag{3.115}$$

respectively. For the cavity in the proposed experiment, we have $\omega D \ll c$. This

condition yields

$$\Delta\omega \approx \omega D \left(\frac{\frac{1}{a^3}}{\frac{1}{a^2} + \frac{1}{h^2}} \right); \qquad \Delta\omega' \approx 0 \tag{3.116}$$

3.3.3 Theoretical Dynamical Casimir Effect Instability

The frequency of modulation of the cavity-frequency is equal to the period of pulse-frequency of the laser (ν_{pulse}) which is chosen to be 5 GHz. Hence in Eq.(3.92) we have, from Eqs.(3.116), $\omega_2 = \Omega + \Delta\omega$, $\omega_1 = \Omega + \Delta\omega'$ and $T = 1/\nu_{pulse}$. Since $\Omega/2\pi = \nu_{pulse}/2$, we have

$$\cos(\gamma) \approx -1 - \frac{1}{2}\left(\frac{\Delta\omega}{\Omega}\right)^2 \tag{3.117}$$

From Eq.(3.92) we have when $|\cos(\gamma)| > 1$, for large number of modulations n, the number of photons as

$$N \sim \exp(2\gamma n), \quad \text{where} \quad \gamma = \left(\frac{\Delta\omega}{\Omega}\right) \tag{3.118}$$

Hence the rate equation can be written as

$$\frac{dN}{dn} = 2\gamma N \tag{3.119}$$

When we take the dissipation into account, we can write this as

$$\frac{dN}{dn} = 2\gamma N - \frac{1}{Q}N \tag{3.120}$$

since, experimentally, it has been verified that the presence of the semiconductor layer doesn't alter the Q-factor of the cavity significantly. For the parameters of the current experiment $\gamma \sim 10^{-3}$ and $Q \sim 10^6$. Hence, we see that, if we run the experiment even for one second, the number of photons produced will be $\sim \exp(10^6)$

which is clearly un-physical. This is the stability issue that needs to be addressed.

3.3.4 Restoration of Theoretical Stability

To begin, let us consider two oscillators with two different frequencies; i.e.

$$H_1 = \frac{1}{2}P^2 + \frac{1}{2}\omega_1^2 Q^2 = \frac{\hbar\omega_1}{2}\left(a_1^\dagger a_1 + a_1 a_1^\dagger\right),$$
$$H_2 = \frac{1}{2}P^2 + \frac{1}{2}\omega_2^2 Q^2 = \frac{\hbar\omega_2}{2}\left(a_2^\dagger a_2 + a_2 a_2^\dagger\right). \tag{3.121}$$

Employing the creation and annihilation operators of the first oscillator into the Hamiltonian of the second oscillator ,($\omega_2 > \omega_1$),

$$H_2 = \frac{\hbar}{2}\left(\omega_1 + \frac{\omega_2^2 - \omega_1^2}{2\omega_1}\right)\left(a_1^\dagger a_1 + a_1 a_1^\dagger\right) + \Delta H_1,$$
$$\Delta H_1 = \left(\frac{\hbar(\omega_2^2 - \omega_1^2)}{4\omega_1}\right)\left(a_1^\dagger a_1^\dagger + a_1 a_1\right). \tag{3.122}$$

The dynamical consequence of a random (noise) frequency shift is thereby a term ΔH_1 which creates or annihilates two quanta.

The issue of stability for a microwave cavity[37] is intimately related to the fact that the modulation is induced by a *pump* which supplies the energy for the induced cavity radiation. One may define a *pump coordinate* η which, in general, is a quantum mechanical operator. In principle, one might mechanically vibrate a wall in the cavity in which case η would be proportional to a mechanical displacement. In practice, changing the frequency by electronic means may well be more efficient[34] .Be that as it may,let us define the coordinate so that

$$\langle\eta(t)\rangle = \frac{\nu^2(t)}{\Omega_0^2}\ , \tag{3.123}$$

wherein $\nu(t) = \Omega_0 + \Delta\omega(t)$ where $\Delta\omega(t)$ is the frequency shifts discussed in Secs.(3.3.3) and (3.3.2) If the quantum pump coordinate exhibits stationary fluctuations

$$\Delta\eta = \eta - \langle\eta\rangle \tag{3.124}$$

with quantum noise

$$\frac{1}{2}\langle\Delta\eta(t)\Delta\eta(t') + \Delta\eta(t')\Delta\eta(t)\rangle = \int_{-\infty}^{\infty} \bar{S}_\eta(\omega)e^{-i\omega(t-t')}d\omega, \tag{3.125}$$

then two photon absorption and two photon emission processes are described by the additional noise Hamiltonian

$$\Delta H = \frac{1}{4}\hbar\Omega_0\left(a^\dagger a^\dagger + aa\right)\Delta\eta. \tag{3.126}$$

The usual mode photon creation and destruction operators are $a^\dagger$ and a, respectively. When the Hamiltonian in Eq.(3.126) is taken to second order in perturbation theory, the resulting energies involve four boson processes which thereby generates multi-photon loop processes.

With the pump coordinate positive and negative frequency spectral functions

$$\begin{aligned}\langle\Delta\eta(t)\Delta\eta(t')\rangle &= \int_{-\infty}^{\infty} S_\eta^+(\omega)e^{-i\omega(t-t')}d\omega,\\ \langle\Delta\eta(t')\Delta\eta(t)\rangle &= \int_{-\infty}^{\infty} S_\eta^-(\omega)e^{-i\omega(t-t')}d\omega,\end{aligned} \tag{3.127}$$

the two photon Fermi golden rule transition rates which follow from Eqs.(3.126) and (3.127) read

$$\begin{aligned}\Gamma^+(n \to n-2) &= \frac{\pi\Omega_0^2}{8}S_\eta^+(\omega = 2\Omega_0)n(n-1),\\ \Gamma^-(n-2 \to n) &= \frac{\pi\Omega_0^2}{8}S_\eta^-(\omega = 2\Omega_0)n(n-1).\end{aligned} \tag{3.128}$$

The pump coordinate also has a noise temperature T_η, which is defined via

$$S_\eta^-(2\Omega_0) = e^{-2\hbar\Omega_0/k_B T_\eta} S_\eta^+(2\Omega_0). \tag{3.129}$$

If there are many photons in the mode, then the net rate of photon absorption is given by

$$\Gamma_{absorption} \simeq \left(\frac{\pi\Omega_0^2\tau_\eta}{4}\right) \tanh\left(\frac{\hbar\Omega_0}{k_B T_\eta}\right) n^2 \quad \text{where} \quad n \gg 1 \ , \qquad \tau_\eta \equiv \bar{S}_\eta(\omega = 2\Omega_0). \tag{3.130}$$

On the other hand, the frequency modulation produces photons at a rate

$$\Gamma_{emmision} \simeq 2\gamma n \quad \text{where} \quad n \gg 1 \ , \tag{3.131}$$

and γ is defined in Eq.(3.118). We may now state the central result of this section:

Theorem 2: *If the pump coordinate pushes the cavity mode into a modulation dynamic Casimir instability, then the quantum noise will stabilize the cavity mode according to the equation*

$$\frac{dn}{dt} = 2(\gamma n - \tilde{\gamma} n^2), \qquad \tilde{\gamma} = \frac{\pi\Omega_0^2\tau_\eta}{8} \tanh\left(\frac{\hbar\Omega_0}{k_B T_\eta}\right). \tag{3.132}$$

The cavity photon occupation number will then saturate according to

$$\bar{n}_{saturate} = \frac{8\gamma}{\pi\Omega_0^2\tau_\eta} \coth\left(\frac{\hbar\Omega_0}{k_B T_\eta}\right) \equiv \frac{k_B T_{sat}}{\hbar\Omega_0} \gg 1. \tag{3.133}$$

An alternative, simpler expression may be derived through the fluctuation dissipa-

tion theorem and the notion of a *relaxation* time[41] for the pump coordinate.

With the response function

$$\chi(\zeta) = \frac{i}{\hbar}\int_o^\infty \langle[\eta(t),\eta(0)]\rangle\, e^{i\zeta t}dt, \tag{3.134}$$

and the fluctuation dissipation theorem

$$\bar{S}_\eta(\omega) = \frac{\hbar}{2\pi}\coth\left(\frac{\hbar\omega}{2k_bT_\eta}\right)\Im m\chi(\omega+i0^+), \tag{3.135}$$

Eq.(3.133) reads

$$\bar{n}_{saturate} = \frac{16\gamma}{\Omega_0^2[\hbar\Im m\chi(2\Omega_0+i0^+)]}. \tag{3.136}$$

The relaxation time $\tau^\dagger$ for the parameter η may be conveniently defined by[41]

$$\chi(0)\tau^\dagger = \lim_{\omega\to 0}\frac{\Im m\chi(\omega+i0^+)}{\omega}, \tag{3.137}$$

so as to obtain

$$\bar{n}_{saturate} \approx \left[\frac{8\gamma}{\Omega_0^3\tau^\dagger\hbar\chi(0)}\right]. \tag{3.138}$$

Eq.(3.138) is our answer for the final number of produced photons.

3.3.5 Calculations and Predictions

In order to render our final answer less abstract[37], consider a proposed experiment[34] and let us provide a concrete numerical estimate for the expected number of photons for their setup. In that proposal, the parameter η describes the metallic conductivity in a semiconductor plate due to a laser beam inducing particle hole pairs. If we let τ_R represent the recombination time taken to annihilate a particle hole pair in the semiconductor and let ω_L represent the laser frequency, then we

estimate that

$$\frac{1}{\tau^\dagger} \approx \frac{\hbar\omega_L\chi(0)}{\tau_R}, \tag{3.139}$$

which implies

$$\bar{n}_{saturate} \approx (\frac{8\gamma}{\Omega_0})(\frac{1}{\Omega_0\tau_R})(\frac{\omega_L}{\Omega_0}). \tag{3.140}$$

The following estimates are reasonable for the proposal[34]

$$(\frac{\gamma}{\Omega_0}) \approx 2 \times 10^{-3}, \tag{3.141}$$

$$(\frac{1}{\Omega_0\tau_R}) \approx 10, \tag{3.142}$$

$$(\frac{\omega_L}{\Omega_0}) \approx 8 \times 10^3, \tag{3.143}$$

so that our estimate is

$$\bar{n}_{saturate} \approx 10^4 \text{ microwave photons.} \tag{3.144}$$

Chapter 4

Conclusions

The instability that might arise when the vacuum field modes couple with matter strongly was examined. A general theoretical framework which studies the instability had been derived. It was shown that the instability is precursor to ferroelectric phase transition and that it is connected with the fact that bound state for a photon cannot exist. It was shown that stability is restored when the system shifts to a polarized phase by radiating out photons. A specific example of a two state, spin0-spin1, ferroelectric system was considered. The critical temperature of the system was calculated. Below the critical temperature it was shown that a double well in the free energy appears and that the stability is achieved by shifting to a new equilibrium coordinate by radiating out photons from vacuum.

Dynamic Casimir effect in the Lagrangian framework and the effect of periodic modulation of the field modes were derived. Description of the novel experiment to detect dynamic Casimir effect was given. Frequency shifts due to the presence of the semiconductor layer was calculated. The result was used to determine photon generation rates and it was shown to exhibit exponential instability. The theoretical framework which restores stability by taking the effect of fluctuations into account

was derived. A concrete numerical estimate of the final number of photons was provided.

Bibliography

[1] H.B.G. Casimir *Proc. K. Ned. Akad. Wet.* **60**, 793 (1948).

[2] H.B.G. Casimir and D. Polder, *Phys. Rev.* **73**, 360 (1948).

[3] A. Erdelyi et al., *"Higher Transcendental Functions"*, Vol. 1, McGraw-Hill, New York, 1953.

[4] D. Kupiszewska, *Phys. Rev.* **A 46**, 2286 (1992).

[5] B.V. Derjaguin, I.I. Abrikosova, E.M. Lifshitz, *Q. Rev.* **10**, 295 (1956).

[6] S.G. Mamaev and N.N. Trunov, *Sov. Phys. J. (USA)* **22**, 51 (1979).

[7] T.H. Boyer, *Phys. Rev.* **174**, 1764 (1968).

[8] M. Bordag, U. Mohideen, and V. M. Mostepanenko, *Phys. Rep.* **205**, 353 (2001).

[9] L.S. Brown and G.J. Maclay, *Phys. Rev.* **184**, 1272 (1969).

[10] J. Schwinger, L.L. DeRaad Jr. and K.A. Milton, *Ann. Phys. (N. Y.)* **115**, (1978)

[11] I.E. Dzyaloshinskii, E.M. Lifshitz and L.P. Pitaevskii, *Sov. Phys. Usp. (USA)* **4**, 153 (1961).

[12] V.B. Bezerra, G.L. Klimchitskaya and V.M. Mostepanenko, *Phys. Rev.* **A 62**, 014102 (2000).

[13] M. Bordag, G.L. Klimchitskaya and V.M. Mostepanenko, *Int. J. Mod. Phys.* **A 10**, 2661 (1995).

[14] M. Bordag, B. Geyer, G.L. Klimchitskaya and V.M. Mostepanenko, *Phys. Rev. Lett.* **85**, 503 (2000).

[15] G.L. Klimchitskaya and Yu.V. Pavlov, *Int. J. Mod. Phys.* **A 11**, 3723 (1996).

[16] M.J. Sparnaay, *Physica* **24**, 751 (1958).

[17] P.H.G.M. van Blokland and J.T.G. Overbeek, *J. Chem. Soc. Faraday Trans.* **74**, 2637 (1978).

[18] S.K.Lamoreaux, *Phys. Rev. Lett.* **78**, 5 (1997).

[19] U.Mohideen and A.Roy, *Phys. Rev. Lett.* **81**, 4549 (1998).

[20] G. Bressi, G. Carugno, R. Onofrio and G. Ruoso, *Phys. Rev. Lett.* **88**, 041804 (2002)

[21] M. Pradeep Ganesh, A. Widom, S. Sivasubramanian and Y. N. Srivastava *Phys. Rev.* **A78**, 052102 (2008)

[22] S. Weinberg, "Quasiparticles and Perturbation Theory", in "Lectures on Particles and Field Theory" Editors: K. Johnson, D.B. Lichtenberg, J. Schwinger and S. Weinberg, p 289, Prentice Hall, Engelwood Cliffs (1965).

[23] N. Levinson, *K. Dan. Vidensk. Selsk. Mat. Fys. Medd.* **25**, 9 (1949).

[24] S. Sivasubramanian, Y. Srivastava and A. Widom, *Int. J of Mod Phys* **B15**, 537 (2001).

[25] S. Sivasubramanian, Y. Srivastava and A. Widom, *Mod Phys Lett* **B16**, 1201 (2002).

[26] S. Sivasubramanian, Y. Srivastava and A. Widom, *J. of Phys. Cond Mat.* **15**, 1109 (2003).

[27] S. Sivasubramanian, Y. Srivastava and A. Widom, *Physica* **A345**, 356 (2005).

[28] E. Fatuzzo and W. J. Merz, "Ferroelectricity", Chapter 2, p 108, North Holland Publishing Company, Amsterdam (1967).

[29] E. Yablonovitch, *Phys. Rev. Lett.*, **62** 1742 (1989).

[30] A. Lambrecht, M. T. Jaekel, and S. Reynaud, *Phys. Rev. Lett.*, **77** 1996.

[31] E. Sassaroli, Y. Srivastava and A. Widom, *Phys. Rev.* **A50**, 1027 (1994).

[32] A. V. Dodonov, E. V. Dodonov and V. V. Dodonov, *Phys. Lett.*, **A317** 378 (2003).

[33] D. A. R. Dalvit, F. D. Mazzitelli and X. Orsi Milln, *J. Phys.*, **A39** 6261 (2006).

[34] C. Braggio, G. Bressi, G. Carugno, C. Del Noce, G. Galeazzi, A. Lombardi, A. Palmieri, G. Ruoso and D. Zanello, *Europhys Lett* **70**, 754 (2005).

[35] V. V. Dodonov and A. B. Klimov, *Phys. Rev.* **A53**, 2664 (1996).

[36] Y. Srivastava and A. Widom, *Phys. Rep.* **148**, 1 (1987).

[37] Y. N. Srivastava, A. Widom, S. Sivasubramanian and M. Pradeep Ganesh, *Phys. Rev.* **A74**, 032101 (2006)

[38] E. Sassaroli, Y. Srivastava and A. Widom, *Nuc. Phys. B(Proc. Suppl.)* **33**, 209 (1993).

[39] W. Magnus and S. Winkler, *"Hill's Equation"*, Dover Publications (2003).

[40] L. D. Landau, L. P. Pitaevskii and E. M. Lifshitz, *"Electrodynamics of Continuous Media"*, Butterworth-Heinemann (1984).

[41] P. C. Martin, *"Measurements and Correlation Functions"*, Gordon and Breach, New York (1968).